ACS OMEGA

Article

Cite This: ACS Omega 2019, 4, 15879−15892

http://pubs.acs.org/journal/acsodf

Early Metal Di(pyridyl) Pyrrolide Complexes with Second Coordination Sphere Arene−π Interactions: Ligand Binding and Ethylene Polymerization

Jessica Sampson,[†,§] Gyeongshin Choi,[†] Muhammed Naseem Akhtar,[‡] E.A. Jaseer,[‡] Rajesh Theravalappil,[‡] Nestor Garcia,[‡] and Theodor Agapie*[,†]

[†]Division of Chemistry and Chemical Engineering, California Institute of Technology, 1200 E California Blvd., Pasadena, California 91125, United States

[‡]Center for Refining and Petrochemicals, King Fahd University of Petroleum and Minerals, Dhahran 31261, Saudi Arabia

Supporting Information

ABSTRACT: Early metal complexes supported by hemilabile, monoanionic di(pyridyl) pyrrolide ligands substituted with mesityl and anthracenyl groups were synthesized to probe the possibility of second coordination sphere arene−π interactions with ligands with potential for allosteric control in coordination chemistry, substrate activation, and olefin polymerization. Yttrium alkyl, indolide, and amide complexes were prepared and structurally characterized; close contacts between the anthracenyl substituents and Y-bound ligands are observed in the solid state. Titanium, zirconium, and hafnium tris(dimethylamido) complexes were synthesized, and their ethylene polymerization activity was tested. In the solid state structure of one of the Ti tris(dimethylamido) complexes, coordination of Ti to only one of the pyridine donors is observed pointing to the hemilabile character of the di(pyridyl) pyrrolide ligands.

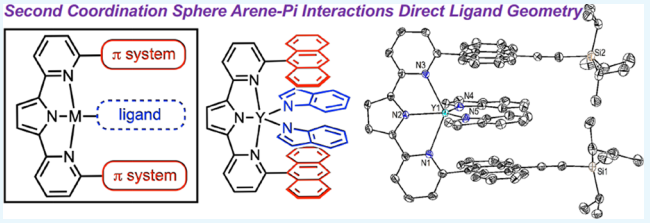

INTRODUCTION

The use of secondary coordination sphere interactions in transition-metal ancillary ligand design has recently emerged as a powerful strategy to modulate the behavior of the resulting complexes and catalysts.[1] Incorporation of hydrogen bond donor groups has been reported to support metal oxo and hydroxo (**A**, Figure 1),[1a,b,2] nitrite activation,[3] CO_2 reduction,[4] and other reactivity.[5] Ligands appended with Lewis acidic moieties have also been reported to promote hydrazine bonding at Fe,[6] reductive CO coupling (**B**),[7] selective alkyne hydrogenation,[8] and other small molecule activation.[9] Lewis base incorporation into the secondary coordination sphere of Fe complexes for N_2 reduction,[10] Ni catalysts for proton reduction (**C**),[11] and Co water oxidation catalysts[12] has reported to change catalyst selectivity and activity. Finally, the use of the combination of pendant Lewis acids and Lewis bases has been reported as a strategy for stabilization of hydrazine binding at V (**D**).[13]

One type of potential interaction, which has been underexplored in the literature, is the use of π interactions through incorporation of pendant π-systems into the ancillary ligands (Figure 2).[14] Terpyridine (terpy) ligands are an example of a ligand framework in which incorporation of such motifs can lead to π−π interactions with additional ligands (Figure 2). Lehn and co-workers demonstrated that incorporation of pyrene groups into the terpy ligand results in formation, upon metal binding, of heteroligated Zn complex **E**, which displays

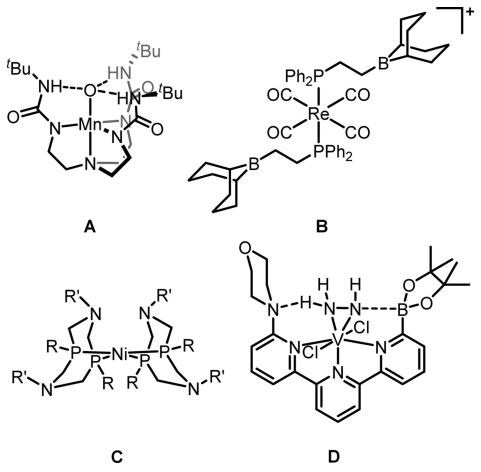

Figure 1. Examples of ligands incorporating secondary coordination sphere effects including hydrogen bond donors (**A**), Lewis acids (**B**), Lewis bases (**C**), and a combination of pendant Lewis acids and bases (**D**).

average distances of 3.50 Å between the pyrene units and the other terpy ligand,[15] and homoligated Cu complex **F** displaying

Received: June 19, 2019
Accepted: August 27, 2019
Published: September 19, 2019

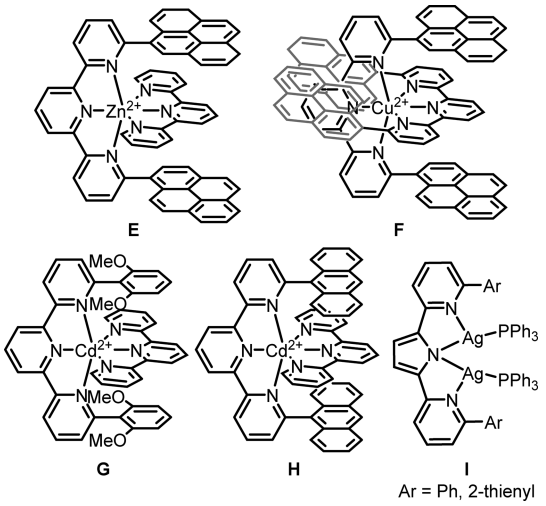

Figure 2. Examples of terpyridine-supported complexes displaying $\pi-\pi$ interactions in the solid state as reported by Lehn and co-workers (**E** and **F**), Chan and co-workers (**G** and **H**), and an example of a crystallographically characterized di(pyridyl) pyrrolide complex bearing arene substituents by Yi and co-workers (**I**).

average distances of 3.50 Å between the pyrene units and the plane of the terpy backbone.[16] Chan and co-workers also demonstrated that incorporation of both 2,6-dimethoxyphenyl, **G**, and anthracenyl, **H**, groups on to the terpy backbone can be used to selectively prepare the heteroligated complexes as a consequence of the favorable electronics of π-stacking in these cases.[17] Despite these and other[18] examples of arene-appended terpy ligands displaying favorable $\pi-\pi$ interactions in the solid state, monoligated complexes, in the absence of additional ligands bearing extended π-systems, do not display parallel aryl substituents in the solid state[19] as a consequence of the central six-membered pyridine donor.

The use of di(pyridyl) ligands bearing a central five-membered substituent was hypothesized to enhance the ability of flanking aryl substituents to interact with incoming substrates in directed X–H bond activation and olefin polymerization (Figure 3). The di(pyridyl) pyrrolide (DPP)

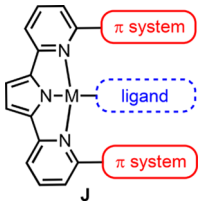

Figure 3. Di(pyridyl)pyrrolide ligands bearing flanking aryl groups for second coordination sphere π interactions with ligands.

backbone, in particular, was thought to be suitable for supported early transition-metal complexes as a consequence of its monoanionic charge. Pyrrolide groups can also bind μ_2 through the nitrogen and η_5 through the pi system.[20] Ti, Zr, and Hf complexes bearing related pyrrolide imine and pyrrolide amine ancillary ligands have been previously shown to be competent for ethylene polymerization.[20n,21] Unsubstituted (dpp) ligands have received attention in the literature as ligands for Ag,[22] Cu,[22,23] Fe,[24] Co,[25] Ru,[26] La,[27] and Pd;[26a,28] however, only those bearing phenyl and 2-thienyl substituents, **I** (Figure 3),[29] have been reported where the DPP substituents could interact with the π-systems of incoming substrates. Such interactions are not observed between the phenyl and 2-thienyl substituents and in the solid-state structures of **I**.

Herein, we report a series of Al, Y, Ti, Zr, and Hf complexes supported by arene-appended di(pyridyl)pyrrolide ligands, which display C–H–π, Cl–π, and $\pi-\pi$ interactions in the solid state. Furthermore, the reactivity of the Ti, Zr, and Hf complexes in ethylene polymerization upon activation with $AlMe_3$ and $[CPh_3][B(C_6F_5)_4]$ is reported.

RESULTS AND DISCUSSION

Aryl-substituted dipyridyl pyrrole proligands were synthesized by Suzuki cross-coupling of the previously reported $(DPP^{Br})H$ (**1**)[30] with the corresponding boronic acid or ester as shown in Scheme 1. 2-Mesitylboronic acid and 9-anthracenylboronic

Scheme 1. Preparation of Aryl-Substituted Di(pyridyl) Pyrrole Proligands through Suzuki Coupling of the Corresponding Aryl Boronic Acid or Ester with the Previously Reported $(DPP^{Br})H$ (1)[30]

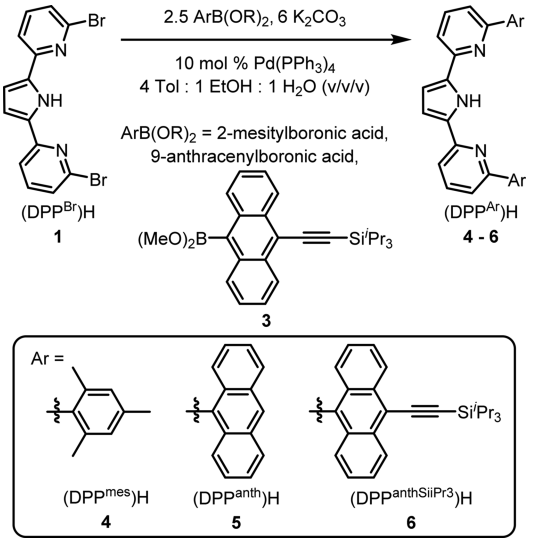

acid were synthesized from the corresponding aryl bromides according to the literature.[31] The 10-tri(*iso*-propyl)silylethyl-substituted anthracene boronic ester (**3**) was prepared from the corresponding bromide (**2**)[32] via lithium–halogen exchange and quenched with trimethylborate. Suzuki coupling of **1** with the corresponding boronic acid or boronic ester affords the aryl-substituted proligands $(DPP^{mes})H$ (**4**), $(DPP^{anth})H$ (**5**), and $(DPP^{anthSiiPr3})H$ (**6**), which were isolated in good yields.

Yttrium bis(tetramethyldisilylazide) complexes were prepared by the reaction of the pyrrole proligands with $Y(N(SiMe_2H)_2)_3(THF)$ in C_6H_6 at elevated temperatures (Scheme 2). In comparison with **7**, **8** features an upfield-shifted Si–H resonance by 3.7 ppm and an upfield-shifted Si–CH_3 resonance by 0.48 ppm, consistent with increased shielding by the more extended π-system of the anthracenyl substituent.[33] X-ray quality crystals of **8** were obtained by slow cooling of a saturated benzene solution (Figure 4). Crystals with two unit cells were observed from the same crystallization; however, initial solutions indicated formation of similar trigonal bipyramidal C_{2V} complexes (τ_5 = 0.01 to 0.05).[34] Two molecules of **8** are observed in the asymmetric

DOI: 10.1021/acsomega.9b01788
ACS Omega 2019, 4, 15879–15892

Scheme 2. Preparation of Bis(tetramethyldisilylazide)yttrium Complexes Supported by the Dipyridylpyrrolide Ligand and Subsequent DPP Transmetallation upon Treatment with AlR_3

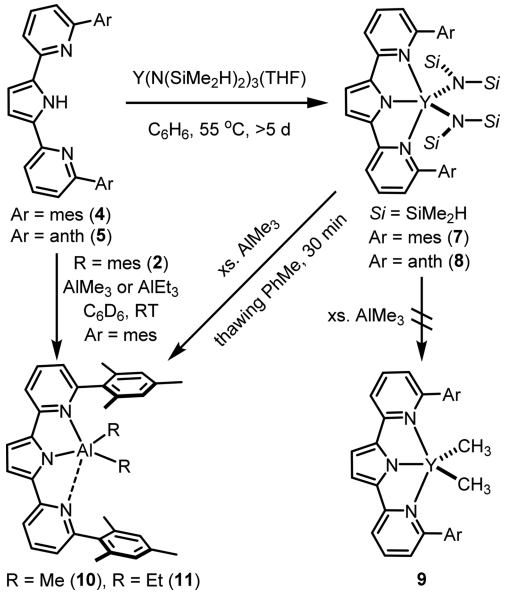

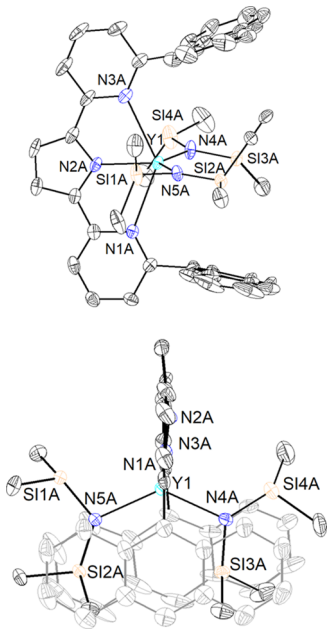

Figure 4. Solid-state structure of **8** with 50% probability anisotropic displacement ellipsoids. Hydrogen atoms and solvent of crystallization are omitted for clarity. The major populations of the disordered tetramethyldisilylazide groups are shown for clarity. Selected bond distances (Å) and angles (°): Y1-N1A 2.671 (4); Y1-N2A 2.266 (3); Y1-N3A 2.648 (4); Y1-N4A 2.214 (3); Y1-N5A 2.249 (3); N1A-Y1-N2A 66.01 (12); N1A-Y1-N3A 132.85 (11); N2A-Y1-N5A 121.66 (12); N2A-Y1-N4A 107.73 (12).

unit of the higher-quality structure; in both, Y is located near equidistant to the pyridine donors, with Y−N(Py) distances in a range of 2.643 (4) to 2.706 (3) Å and Y−N(pyrrole) distances in a range of 2.266 (3) to 2.245 (3) Å. Angles of 33.4° and 31.4° are observed between the anthracenyl groups; such distortion is likely a consequence of the size of the tetramethyldisilylazide groups.

Treatment of **7** with $AlMe_3$ or $AlEt_3$ leads to formation of new metal alkyl-containing species. The product of the reaction of **7** with $AlEt_3$ was identified as the four-coordinate diethylaluminum complex **10** (τ_4 = 0.88; Figure 5)[35] by X-ray

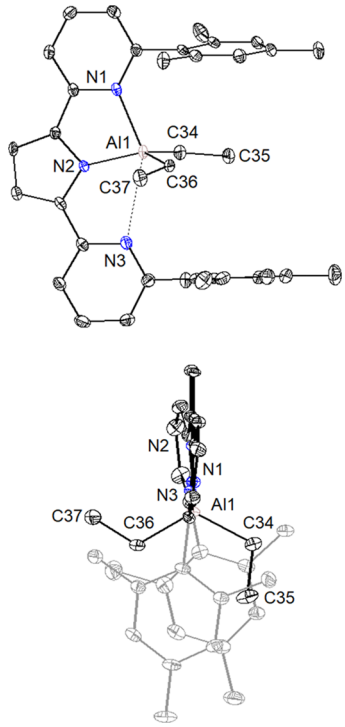

Figure 5. Solid-state structure of **11** with 50% probability anisotropic displacement ellipsoids. Hydrogen atoms are omitted for clarity. Selected bond distances (Å) and angles (°): Al1-N1 2.098 (2); Al1-N2 1.8922 (19); Al1-C34 1.977 (2); Al1-C36 1.957 (2); N1-Al1-N2 81.03 (8); N2-Al1-C36 117.90 (10); N2-Al1-C36 117.12 (9).

crystallography and independent synthesis. A distance of 2.885 (2) Å from Al (1) to N (3) of the free pyridine is observed, which is within the sum of van der Waals radii (3.91 Å).[36] Comparison of the ^{1}H NMR spectra of the products of the reaction of **7** with $AlMe_3$ and $AlEt_3$ with the products of the reactions of **4** with $AlMe_3$ and $AlEt_3$ indicates formation of the same species in both reactions (Figures S13 and S14). Such ancillary ligand transmetallation from Y to Al has been observed in a number of other systems including in related iminopyrrolide complexes.[37]

Reaction of **6** with $Y(CH_2SiMe_3)_3(THF)_2$ in thawing hexanes over 40 min affords a red-brown species with NMR features consistent with C_{2V} $Y(CH_2SiMe_3)_2(THF)$ complex **12** (Scheme 3). An upfield-shifted doublet is observed in the ^{1}H NMR spectrum at −2.33 ppm ($^2J_{YH}$ = 2.4 Hz), which is assigned to the methylene protons of the CH_2SiMe_3 groups; the CH_2SiMe_3 resonance is observed at 29.41 ppm ($^1J_{YC}$ = 31.0 Hz) in the ^{13}C NMR. X-ray quality crystals were grown by slow evaporation of a pentane solution of the complex at −35 °C (Figure 6). The DPP ligand binds meridionally with a short Y−N(pyrrolide) distance of 2.259 (2) Å and two long Y−N(pyr) distances of 2.591 (2) and 2.563 (2) Å. The two CH_2SiMe_3 groups are located trans to one another, and the coordination sphere is filled with THF bound between the two anthracenyl substituents. Distances of 3.64 and 3.46 Å are observed between the oxygen of the bound THF and the planes of the two anthracenyl substituents, consistent with C−

DOI: 10.1021/acsomega.9b01788
ACS Omega 2019, 4, 15879−15892

Scheme 3. Synthesis and Reactivity of (Dialkyl)yttrium Complex 12

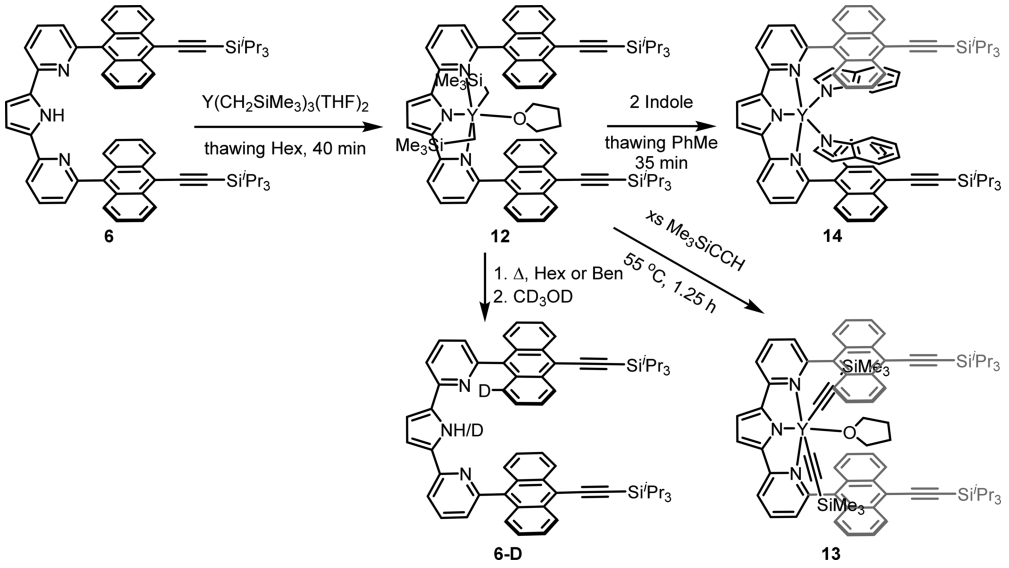

H−π interactions between the THF and the ligand substituents.

Reaction of **12** with excess trimethylsilylacetylene upon heating to 55 °C for 1.25 h affords a new C_{2V} symmetric species with NMR features consistent with **13**. In comparison with the starting material, **13** features an upfield-shifted pyrrole resonance at 6.96 ppm in the ^{1}H NMR and broad resonances at 1.48 and 1.00 ppm corresponding to the bound THF group. The trimethylsilyl resonance of the bound acetylide is shifted to 0.04 ppm from 0.11 ppm in the free alkyne, while the ^{13}C resonances of the C≡C-SiMe$_3$ unit are observed as doublets at 171.37 ppm ($^1J_{YC}$ = 48.83 Hz) and 108.38 ppm ($^2J_{YC}$ = 8.42 Hz). Reaction of **12** with aromatic substrates such as benzene, phenanthrene, and 2,3,4,5,5-pentafluorotoluene was attempted; however, decomposition with loss of SiMe$_4$ and THF was observed to initially form a species with a set of two doublets of doublets centered at −2.07 and − 2.53 ppm ($^1J_{HH}$ = 11.6 Hz, $^2J_{YH}$ = 3.3 Hz) corresponding to a species bearing a single CH$_2$SiMe$_3$ group with loss of symmetry between the two pyridine donors. MeOD quench of this species leads to deuterium incorporation into the DPP ligand as shown in Scheme 3.

12 reacts with 2 equiv of indole to release THF and 2 equiv of SiMe$_4$ and affords the bis(indolide) complex **14**, which was confirmed by X-ray crystallography (Figure 7). The NMR features of this complex are broadened in comparison with **12** and **13**. This broadness could be a consequence of the interaction of the indolide substrates with the extended π-systems of the anthracenyl substituents. In the solid state, this distorted square pyramidal complex (τ_5 = 0.07) displays an average distance of 3.38 Å between the nitrogen atoms of the indolide ligands and the plane of the anthracenyl substituents, consistent with π−π interaction. The six-membered rings of the indolide ligands are positioned away from the Y center and toward the anthracenyl substituents, suggesting that formation of the π−π interactions is favored in comparison with formation of less sterically congested complexes. As in the structure of **12**, **14** exhibits longer Y(1)−N(Py) distances (2.516 (2) and 2.518 (2) Å) in comparison with a shorter Y(1)−N (2) distance of 2.260 (2) Å. Similar Y(1)−N(Ind) distances of 2.238 (3) an 2.245 (3) Å are observed.

Reaction of **4** or **5** with ZrCl$_4$ upon in situ ligand deprotonation with KHMDS afforded complexes with exceedingly low solubility, leading to poor reproducibility of the syntheses; however, grow crystals are suitable for X-ray diffraction of the six-coordinate complex zirconium trichloride complex **15** (Figure 8) from this route. This complex features two long Zr-Py distances of 2.392 (1) and 2.368 (1) Å with a relatively short Zr-pyrrolide distance of 2.148 (1) Å. The three Cl ligands are located at similar distances from Zr (1), in a range of 2.4006 (4) to 2.4273 (6) Å. The chloride ligand trans to the pyrrolide donor is located between the two anthracenyl ligand substituents with distances of 3.19 and 3.23 Å between the chloride and the planes of the anthracene groups. These distances are within the sum of the van der Waals radii (3.4 Å) and are consistent with halogen−π interactions.[38]

Due to the low solubility of this and other targeted chloride complexes and difficulties with complex isolation, more soluble complexes were targeted. Reaction of M(NMe$_2$)$_4$ (M = Ti, Zr, Hf) precursors with the pyrrole proligands in toluene at room temperature affords the corresponding tris(dimethylamido) complexes in good yields (Scheme 4). All tris(dimethylamido) complexes, as isolated, feature a single dimethylamido resonance with equivalent pyridines and equivalent aromatic ligand substituents by ^{1}H and ^{13}C NMR, consistent with fast exchange between free and bound pyridine groups on the NMR timescale at room temperature. Upfield-shifted NMe$_2$ resonances are also observed for the complexes bearing anthracene substituents as compared with complexes bearing mesityl substituents ($\Delta\delta_{NMe}$(Ti) = 0.38; $\Delta\delta_{NMe}$(Zr) = 0.48; $\Delta\delta_{NMe}$(Hf) = 0.47) consistent with increased shielding by the more extended anthracenyl π-system.

Crystals suitable for X-ray diffraction could be grown for (DPP^{mes})Ti(NMe$_2$)$_3$ (**16**, Figure 9). This crystallizes with two molecules in the asymmetric unit; however, both feature five-coordinate Ti centers with distorted trigonal bipyramidal geometry (τ_5 = 0.74 and 0.73), with a free pyridine group. Consistent with other structures, both Ti centers are located closer to the pyrrolide N as compared with the pyridine N (2.1070 (10) and 2.1054 (11) Å vs 2.3658 (11) and 2.3792 (11) Å). The dissociated pyridine arm is rotated away from the Ti center with Ti−N distances of 5.0 to 5.1 Å and an angle of

DOI: 10.1021/acsomega.9b01788
ACS Omega 2019, 4, 15879−15892

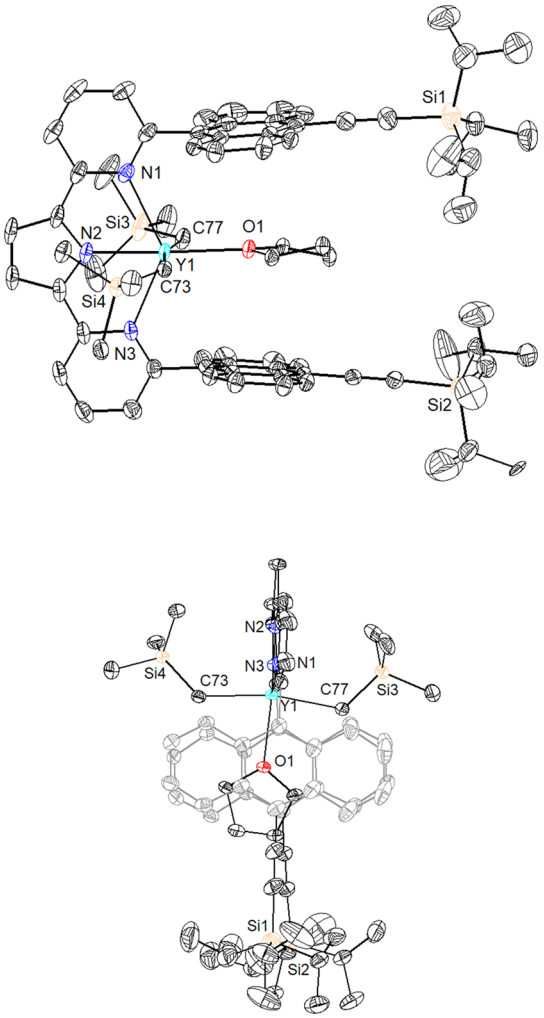

Figure 6. Solid-state structure of **12** with 50% probability anisotropic displacement ellipsoids. Hydrogen atoms are omitted for clarity. Selected bond distances (Å) and angles (°): Y1-N1 2.563 (2); Y1-N2 2.259 (2); Y1-N3 2.590 (2); Y1-C73 2.465 (2); Y1-C77 2.470 (2); Y1-O1 2.4476(17); N1-Y1-N3 131.78 (7); N1-Y1-N2 66.12 (7); N2-Y1-N3 65.86 (7); N2-Y1-O1 176.38 (6); N2-Y1-C73 94.77 (7); N2-Y1-C77 97.48 (8).

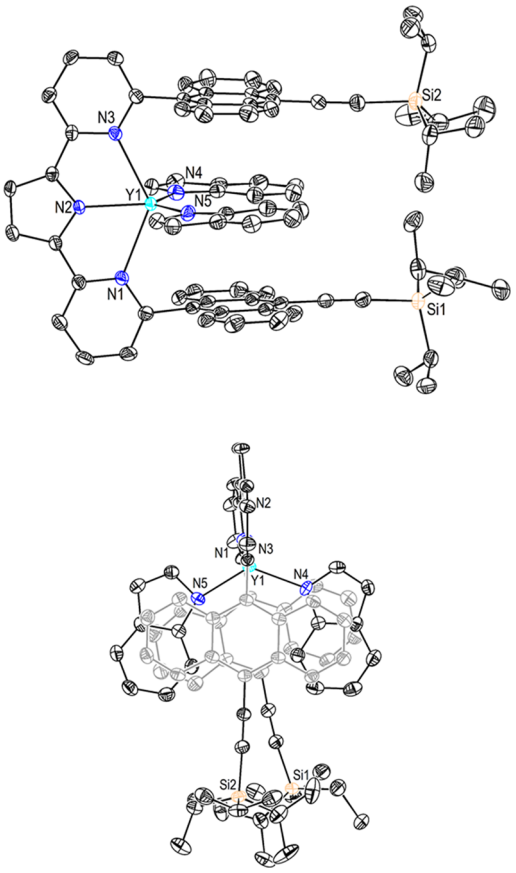

Figure 7. Solid-state structure of **14** with 50% probability anisotropic displacement ellipsoids. Hydrogen atoms are omitted for clarity. Selected bond distances (Å) and angles (°): Y1-N1 2.518 (2); Y1-N2 2.260 (2); Y1-N3 2.516 (2); Y1-N4 2.245 (3); Y1-N5 2.238 (3); N1-Y1-N2 66.34 (8); N1-Y1-N3 131.97 (7); N2-Y1-N4 114.42 (10); N2-Y1-N5 117.89 (10).

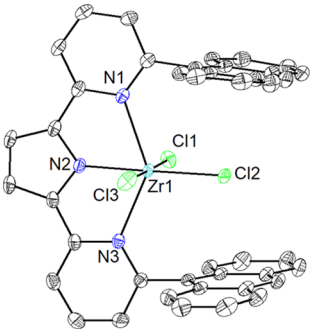

Figure 8. X-ray structure of **15** with 50% probability anisotropic displacement ellipsoids. Hydrogen atoms are omitted for clarity. Selected bond distances (Å) and angles (°): Zr1-N1 2.3685 (11); Zr1-N2 2.1478 (11); Zr1-N3 2.3921 (11); Zr1-Cl1 2.4189 (4); Zr1-Cl2 2.4006 (4); Zr1-Cl3 2.4273 (4); N1-Zr1-N2 69.15 (4); N1-Zr1-N3 137.59 (4); N2-Zr1-Cl1 89.69 (3); N2-Zr1-Cl2 179.24 (3); N2-Zr1-Cl3 89.61 (3).

28° between the plane of the unbound pyridine and the bound pyrrolide and pyridine. The Ti centers are both located out of the plane of the bound pyrrolide and pyridine donors by 0.87 Å. A similar metal geometry was observed by X-ray crystallography by Bochmann and co-workers in their Zr tris(dimethylamido) complex supported by the bis(imino)-pyrrolide ligand.[21a]

Based on the crystallographically characterized complexes supported by the aryl-substituted DPP ligands, coordination of small and/or flat ligands to metal centers supported by these ancillary ligands leads to the formation of interactions with the DPP mesityl and anthracenyl substituents. Distances in the range of 3.3 to 3.6 Å are observed between ligands and aryl substituents, within the sum of the van der Waals radii. As demonstrated in the solid-state structure of **8**, coordination of the larger (tetramethyldisilylazide) ligands leads to significant distortion of the anthracenyl substituents away from coplanarity. As a consequence of the large bite angle of the DPP ligand, ready ligand activation can occur in the case of Y and, with the Ti, Zr, and Hf tris(dimethylamido) complexes, exchange of free and bound pyridine arms is rapid at room temperature, although coordination to only two donors is favored in the solid-state structure of **16**. This may indicate that the use of these arene-substituted DPP ligands with larger metals could lead to compounds more competent for intermolecular substrate activation by disfavoring pyridine dissociation. From the solid-state structure of **14**, interaction of

DOI: 10.1021/acsomega.9b01788
ACS Omega 2019, 4, 15879−15892

Scheme 4. Synthesis of Tris(dimethylamido) Ti, Zr, and Hf Complexes

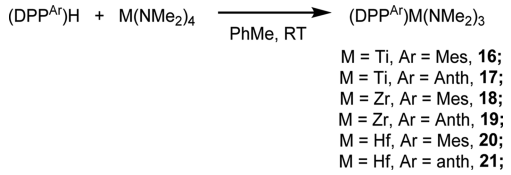

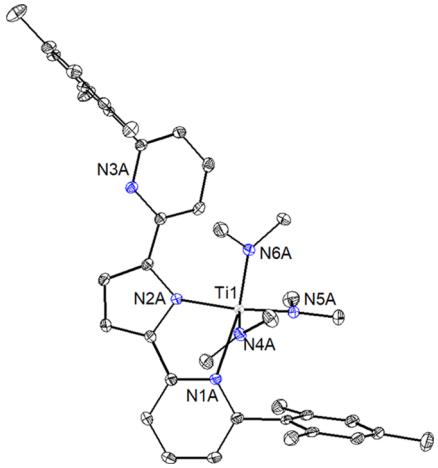

Figure 9. Solid-state structure of **16** with 50% probability anisotropic displacement ellipsoids. Hydrogen atoms are omitted for clarity. One of two molecules in the asymmetric unit is shown for clarity. Selected bond distances (Å) and angles (°): T1-N1A 2.3658 (11); T1-N2A 2.1054 (11); T1-N4A 1.8864 (12); T1-N5A 1.9143 (12); T1-N6A 1.9358 (11); N1A-T1-N2A 74.09 (4); N2A-Ti1-N4A 126.72 (5); N2A-Ti1-N5A 117.82 (5); N2A-Ti1-N6A 96.29 (5).

substrates bearing extended aromatic substituents with the flanking anthracene substituents is favored; however, competition with formation of lower coordinate number species and facile ligand activation limits applicability in the current series of complexes.

The tris(dimethylamido) complexes **16**, **17**, **18**, **19**, and **20** were evaluated for their activity in the homopolymerization and in the copolymerization of ethylene and 1-hexene. In initial small-scale reactions with **18**, no activity was observed in toluene using MMAO-12 and minimal activity was observed in chlorobenzene (Table S1, entries 1 and 2). The best activity from **18** was observed using a mixture of $AlMe_3$ and $[CPh_3][B(C_6F_5)_4]$ as an activator and cocatalyst (740 g $mmol_M^{-1}$ h^{-1}, Table S1, entry 3). Between the mesityl- and anthracenyl-substituted Zr and Ti complexes under $AlMe_3$/$[CPh_3][B(C_6F_5)_4]$ activation conditions, no activity differences were observed; however, the activity did vary depending on the nature of the metal. In all cases, very broad molecular weight distributions were observed, which is likely a consequence of processes including chain transfer to aluminum, multiple di(pyridyl) pyrrolide binding modes (Figure 10), and different degrees of dimethylamido group substitution. The lack of effect from the aryl substituents could indicate that interaction between the 1-hexene and ethylene monomers and the mesityl and anthracenyl substituents does not substantially alter catalyst behavior; alternatively, this could indicate that these groups are not positioned so as to interact with the incoming monomers in the active catalyst(s). The differences in activity between the Ti, Zr, and Hf complexes could be indicative of

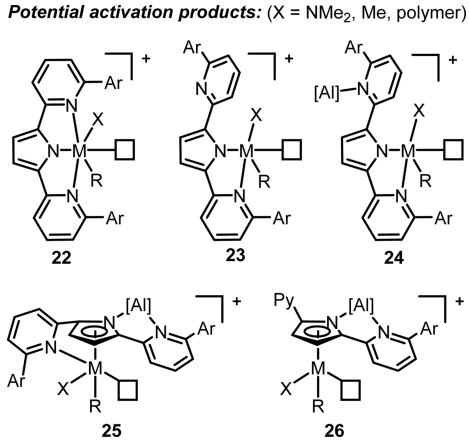

Figure 10. Potential products from the activation of (DPP)M-$(NMe_2)_3$ complexes with $AlMe_3$ and $[CPh_3][B(C_6F_5)_4]$.

different species being formed upon activation of these complexes (Figure 10); with the smaller Ti, a lower coordination complex is formed due to single pyridine binding resulting in a more active species that produces higher-molecular-weight products, whereas with the larger metals, formation of less active species is favored.

CONCLUSIONS

In summary, a series of early metal alkyl, amide, indolide, and acetylide complexes supported by mesityl- and anthracenyl-substituted di(pyridyl)pyrrolide ligands were synthesized, and the effects of the extended π-substituents on their NMR and structural features were examined. As a consequence of the anthracenyl substituents, significantly upfield-shifted NMR resonances are observed for the amide resonances on Y, Ti, Zr, and Hf complexes. The anthracenyl substituents are observed to have close contacts with indolide, THF, chloride, and tetramethyldisilylazide substituents and long metal-pyridine distances where coordination of both pyridine donors is favored. In the structurally characterized tris-(dimethylamido)titanium complex, however, dissociation of one pyridine is observed in the solid state to accommodate a closer metal-pyridine distance. The ethylene polymerization behavior of the tris(dimethylamido) group IV complexes was tested, and Ti and Zr complexes were found to be competent for ethylene polymerization when activated with $AlMe_3$ and $[CPh_3][B(C_6F_5)_4]$, although the resulting polymers displayed very broad molecular weight distributions, which is proposed to result from both from chain transfer to Al and the formation of multiple species under these activation conditions.

EXPERIMENTAL SECTION

General Comments. All air- and water-sensitive compounds were manipulated under N_2 using standard Schlenk or glovebox techniques. Solvents for air- and moisture-sensitive reactions were dried by the method of Grubbs.[39] Trimethylsilylacetylene, chlorobenzene, and 1-hexene were stirred over CaH_2 for upward of 72 h, vacuum transferred or distilled, and run over activated alumina prior to use. **1**,[30] 2-mesitylboronic acid,[31a] 9-anthracenylboronic acid,[31b] **2**,[32] $Zr(NMe_2)_4$,[40] $Hf(NMe_2)_4$,[41] $Y(CH_2SiMe_3)_3(THF)_2$,[42] and $Y(N(SiMe_2H)_2)_3(THF)_2$[43] were prepared according to literature procedures. $[CPh_3][B(C_6F_5)_4]$ was purchased from Strem and used without further purification. Methylaluminoxane (10% in

DOI: 10.1021/acsomega.9b01788
ACS Omega 2019, 4, 15879−15892

toluene), $AlMe_3$, and $AlEt_3$ were purchased from Sigma-Aldrich and used without further purification. Deuterated solvents were purchased from Cambridge Isotopes Laboratories, Inc. $CDCl_3$ was used without further purification; C_6D_6 was distilled from purple Na/benzophenone ketyl and stored over 4 Å molecular sieves prior to use. ^1H and ^{13}C spectra were recorded on Varian INOVA-400, Bruker Cryoprobe 400, and Bruker 400 spectrometers. ^1H and ^{13}C chemical shifts are reported relative to residual solvent resonances. Elemental analysis was performed on a PerkinElmer 2400 CHNS/O analyzer, and samples were taken from representative batches prepared in an N_2-filled glovebox, unless otherwise noted.

Preparation of 3. A Schlenk flask was charged with **2** (4.6167 g, 10.55 mmol) and THF (400 mL) and cooled to −78 °C with a dry-ice/acetone bath. *n*BuLi (4.2 mL, 10.5 mmol) was added over the course of several minutes, and then $B(OMe)_3$ (3.5 mL, 31.4 mmol) was added in one portion after 1 h. The reaction was allowed to come to room temperature over 8 h and then quenched by addition of 2 N HCl. Volatiles were removed under reduced pressure, and the residue was taken up in DCM and washed with water and brine, dried with $MgSO_4$, filtered, and evaporated. Purification by column chromatography with an initial eluent of 10% EtOAC in hexanes allowed separation of the major impurities, and the desired material was eluted with 10% MeOH in DCM to afford a mixture of the dimethyl borate, methyl borate, and boronic acid, which was used for the next Suzuki coupling without further purification (3.273 g, 7.603 mmol, 77%). ^1H NMR (400 MHz, $CDCl_3$, δ): 8.66 (m, 2H, anth), 7.86 (m, 2H, anth), 7.60−7.50 (m, 4H, anth), 3.61 (s, 6H, $B(OCH_3)_2$), 1.27 (m, 21H, Si*i*Pr$_3$). ^{13}C NMR (101 MHz, $CDCl_3$, δ): 134.16, 133.01, 132.46, 128.65, 127.63, 126.65, 126.14, 118.64, 103.53 (−C≡C−), 103.42 (−C≡C−), 52.96 ($B(OCH_3)_2$), 19.05 (Si(CH-$(CH_3)_2)_3$), 11.66 (Si$(CH(CH_3)_2)_3$). HRMS (FAB+) for $C_{27}H_{35}O_2BSi$, 430.2499; found, 430.2501.

Preparation of 4. A Schlenk tube was charged with **1** (0.9217 g, 2.432 mmol), 2-mesitylboronic acid (1.0188 g, 6.212 mmol), K_2CO_3 (2.2078 g, 15.975 mmol), toluene (24 mL), ethanol (6 mL), and water (6 mL) and then degassed by three freeze-pump-thaw cycles at −78 °C. The flask was backfilled with N_2, then $Pd(PPh_3)_4$ (0.147 g, 0.127 mmol) was added against strong N_2 counterflow, and the flask was heated to 70 °C overnight. Aqueous and organic layers were separated, and the aqueous layer extracted twice with DCM. The combined organic layers were washed with water and brine, then dried with $MgSO_4$, filtered, and evaporated. Column chromatography in 10:1 hexanes/EtOAc (v/v) afforded the desired compound as a pale yellow solid (0.7873 g, 1.720 mmol, 71% yield). ^1H NMR (400 MHz, $CDCl_3$, 25 °C, δ): 10.43 (s, 1H, N*H*), 7.69 (t, *J* = 7.7 Hz, 2H, Py), 7.55 (dd, *J* = 8.0, 1.1 Hz, 2H, Py), 6.99−6.95 (m, 10H, mes and Py), 6.86 (d, *J* = 2.6 Hz, 2H, pyrr), 2.36 (s, 6H, mesCH_3), 2.07 (s, 12H, mesCH_3). ^{13}C NMR (101 MHz, $CDCl_3$, 25 °C, δ) 159.5 (py), 150.1 (pyrr), 138.3 (mes), 137.5 (mes), 136.5 (Py), 136.1 (mes), 133.7 (Py), 128.3 (mes), 121.8 (Py), 116.4 (Py), 109.2 (pyrr), 21.3 (mesCH_3), 20.39 (mesCH_3). HRMS (FAB+) for $C_{32}H_{32}N_3$ (M + H), 458.2596; found, 458.2609.

Preparation of 5. A Schlenk tube was charged with **1** (1.034 g, 2.729 mmol), 9-anthracenyl boronic acid (1.514 g, 6.820 mmol), K_2CO_3 (2.620 g, 18.95 mmol), toluene (54 mL), ethanol (14 mL), and water (14 mL) and then degassed by three freeze-pump-thaw cycles at −78 °C. The flask was backfilled with N_2, and then $Pd(PPh_3)_4$ (0.335 g, 0.290 mmol) was added against strong N_2 counterflow. The flask was sealed and heated to 70 °C for 15 h. Upon cooling to room temperature, the reaction was filtered and a yellow solid was collected. This was subsequently washed with methanol and then dried under vacuum to afford the desired compound (1.530 g, 2.667 mmol, 98% yield). ^1H NMR (400 MHz, DMSO-d_6, 25 °C, δ): 11.02 (s, 1H, N*H*), 8.65 (s, 2H, anth), 8.11 (d, *J* = 8.4 Hz, 4H), 8.04 (dd, *J* = 8.1, 1.2 Hz, 2H, Py), 7.99 (t, *J* = 7.7 Hz, 2H, Py), 7.57−7.53 (m, 4H, anth), 7.47 (ddd, *J* = 8.2, 6.6, 1.2 Hz, 4H, anth), 7.36 (ddd, *J* = 8.8, 6.5, 1.3 Hz, 4H, anth), 7.31 (dd, *J* = 7.2, 1.1 Hz, 2H, Py), 6.99 (d, *J* = 2.3 Hz, 2H, pyrr). ^{13}C NMR (101 MHz, DMSO-d_6, 25 °C, δ): 157.0, 150.5, 137.8 (CH of py), 135.5, 135.4, 135.0, 134.1, 133.5, 131.3, 129.8, 129.7, 129.0 (anth), 128.8, 127.6 (anth), 127.23, 126.5 (anth), 126.1 (anth), 125.8 (anth), 124.5 (Py), 118.1 (Py), 111.2 (pyrr). HRMS (FAB+) for $C_{42}H_{28}N_3$, 574.2283; found, 574.2279.

Preparation of 6. A Schlenk tube was charged with **1** (0.5170 g, 1.364 mmol, 1 equiv), K_2CO_3 (1.1641 g, 8.422 mmol, 6.2 equiv), **3** (1.377 g, 3.42 mmol 2.5 equiv), toluene (35 mL, 10 mL/mmol), ethanol (8 mL, 2.5 mL/mmol), and water (8 mL, 2.5 mL/mmol). This was degassed by three freeze-pump-thaw cycles, and then $Pd(PPh_3)_4$ (0.203 g, 0.176 mmol, 0.129 equiv.) was added against strong N_2 counterflow. The flask was sealed, heated to 70 °C for 9 h, then cooled to room temperature, and diluted with DCM and water. The organic phase was separated, washed with water and brine, then dried with $MgSO_4$, and filtered, and volatiles were removed under reduced pressure. The crude reaction was dry-loaded with SiO_2 and purified by column chromatography in 10% benzene and 20% DCM in hexanes to afford the desired product as a bright yellow solid (1.1 g, 1.2 mmol, 88% yield). ^1H NMR (500 MHz, $CDCl_3$, δ): 10.24 (s, 1H, N*H*), 8.6 (d, *J* = 8.8 Hz, 4H, anth), 7.79 (t, *J* = 7.9 Hz, 2H, Py), 7.71 (d, *J* = 7.9 Hz, 2H), 7.53 (d, *J* = 8.7 Hz, 4H, anth), 7.46 (t, *J* = 7.5 Hz, 4H, anth), 7.24 (t, *J* = 7.4 Hz, 4H, anth), 7.13 (d, *J* = 7.1 Hz, 2H, Py), 6.95 (d, *J* = 1.9 Hz, 2H, pyrr), 1.34−1.25 (m, 42H, Si*i*Pr$_3$). ^{13}C NMR ($CDCl_3$, 101 MHz, δ): 157.51 (Py), 150.41 (Py), 136.57 (Py), 133.68 (pyrr), 132.66 (anth), 129.59 (anth), 127.04 (anth), 126.86 (anth), 126.41 (anth), 125.86 (anth), 124.10 (Py), 118.58 (anth), 117.42 (Py), 109.89 (pyrr), 108.59 (anth), 103.60 (−C≡C−), 103.18 (−C≡C−), 19.05 (SiCH$(CH_3)_2$), 11.65 (SiC$H(CH_3)_2$). HRMS (FAB+) (M + H)-H2 for $C_{64}H_{66}N_3Si_2$, 932.4795; found, 932.4796.

Preparation of 7. A Schlenk tube was charged in the glovebox with $Y(N(SiMe_2H)_2)_3(THF)_2$ (0.2902 g, 0.4605 mmol), **4** (0.2105 g, 0.4599 mmol, 1 equiv), and benzene (9 mL), then sealed, and heated to 75 °C for 5 days. Volatiles were removed under reduced pressure, then the resulting solids were triturated with hexanes, and solids were collected by filtration to afford the desired compound as a bright yellow solid (0.1483 g, 0.1830 mmol, 40% yield). ^1H NMR (C_6D_6, 400 MHz, δ): 7.27 (dd, *J* = 1.2, 8.1 Hz, 2H, Py), 6.98 (t, *J* = 7.8 Hz, 2H, Py), 6.90 (s, 2H, pyrr), 6.86 (s, 4H, mes), 6.29 (dd, *J* = 1.2, 7.5 Hz, Py), 4.34 (sept, *J* = 2.9 Hz, 4H, Si*H*$(CH_3)_2$), 2.21 (s, 12H, mesCH_3), 2.16 (s, 6H, mesCH_3), 0.11 (d, *J* = 3.0 Hz, 24H, SiH$(CH_3)_2$). ^{13}C NMR (C_6D_6, 101 MHz, δ) 161.69 (Py), 157.12 (Py), 141.73 (pyrr), 138.58 (Py), 138.11 (mes), 137.40 (mes), 136.37 (mes), 129.65 (mes), 122.39 (Py), 118.07 (Py), 112.16 (pyrr), 22.20 (mesCH_3), 21.15 (mesCH_3), 3.78 (SiH$(CH_3)_2$). Satisfactory elemental analysis could not be obtained for this complex.

DOI: 10.1021/acsomega.9b01788
ACS Omega 2019, 4, 15879−15892

Preparation of 8. A J-Young tube was charged in the glovebox with $Y(N(SiMe_2H)_2)_3(THF)_2$ (16.8 mg, 0.0267 mmol), **5** (14.8 mg, 0.0258 mmol), and C_6D_6 (0.5 mL), then sealed, and heated to 75 °C for 5 days. Volatiles were removed in vacuo. Recrystallization from benzene−pentane at room temperature afforded the desired compound as a yellow-orange solid (12.3 mg, 0.0133 mmol, 52% yield). Note that this compound was isolated with a small amount (ca. 12% by ^{1}H NMR integration) of another $N(SiHMe_2)_2$-containing species from which it could not be separated. X-ray quality crystals were grown by slow cooling of the crude reaction mixture in a J-Young tube. ^{1}H NMR (C_6D_6, 400 MHz, δ): 8.15 (s, 2H, anth), 7.78−7.73 (m, 8H, anth), 7.44 (dd, J = 8.1, 1.2 Hz, 2H, Py), 7.22−7.13 (m, 12H, anth), 7.08 (s, 2H, pyrr), 6.95 (dd, J = 8.1, 7.6 Hz, 2H, Py), 6.25 (dd, J = 7.4, 1.2 Hz, 2H), 3.73.74 (sept, J = 2.7 Hz, 4H, $N(SiH(CH_3)_2)_2$), −0.48 (d, J = 2.9 Hz, 24 H, $N(SiH(CH_3)_2)_2$). ^{13}C NMR (C_6D_6, 101 MHz, δ): 160.03 (Py), 157.13 (Py), 141.89 (pyrr), 138.29 (Py), 134.47 (anth), 132.14 (anth), 131.66 (anth), 129.12 (anth), 129.04 (anth), 127.55 (anth), 126.68 (anth), 125.61 (anth), 125.13 (Py), 118.82 (Py), 112.63 (pyrr), 2.92 ($SiH(CH_3)_2$). Satisfactory elemental analysis could not be obtained for this complex.

Preparation of 11. For method A, a J-Young tube was charged with **4** (19.2 mg, 0.0420 mmol) and $AlEt_3$ (5.8 μmol, 0.0423 mmol) in C_6D_6 (0.5 mL), then sealed, and inverted. Gas evolution was observed upon mixing, and yellow crystals were observed upon standing (quantitative yield by NMR). For method B, $AlEt_3$ (67 μL, 0.49 mmol) was added to a thawing solution of **7** (39.7 mg, 0.0490 mmol) in PhMe (2 mL) and stirred for 30 min. Volatiles were removed under reduced pressure, and the resulting yellow oil was triturated with pentane and filtered over Celite. Extraction of the remaining yellow solids with benzene afforded the desired complex as a yellow solid (22.2 mg, 0.0410 mmol, 84%). X-ray quality crystals were grown by vapor diffusion of pentane into a toluene solution of the complex in toluene at −35 °C. Elemental analysis was performed on the material prepared by method A. ^{1}H NMR (C_6D_6, 400 MHz, δ): 7.19 (dd, J = 8.0, 1.1 Hz, 2H, Py), 7.05−6.98 (m, 4H, Py and pyrr), 6.70 (s, 4H, mes), 6.41 (dd, J = 7.4, 1.1 Hz, 2H, Py), 2.07 (s, 12H, mesCH_3), 1.94 (s, 6H, mesCH_3), 0.79 (t, J = 8.1 Hz, 6H, $AlCH_2CH_3$), 0.00 (q, J = 8.1 Hz, 4H, $AlCH_2CH_3$). ^{13}C NMR (C_6D_6, 101 MHz, δ): 159.89 (Py), 153.22 (Py), 139.73 (pyrr), 138.18 (Py), 138.05 (mes), 136.64 (mes), 136.23 (mes), 128.44 (mes), 121.42 (Py), 116.49 (Py), 111.81 (pyrr), 21.06 (mesCH_3), 20.53 (mesCH_3), 9.55 ($AlCH_2CH_3$), −0.64 ($AlCH_2CH_3$). Anal calcd. for $C_{36}H_{40}N_3Al$: C, 79.82; H, 7.44; N, 7.76. Found: C, 79.98; H, 7.51; N, 7.81.

Preparation of 12. A vial was charged with $Y(CH_2SiMe_3)_3(THF)_2$ (83.2 mg, 0.168 mmol, 1.2 equiv), a stirbar, and hexanes (2 mL) and frozen in the glovebox cold well. A separate vial was charged with **6** (132.0 mg, 0.1413 mmol, 1 equiv) and hexanes (3 mL) and frozen; the thawing solution of **6** was added to the top of the stirred Y solution. The resulting suspension was stirred for 40 min until warmed and then filtered over Celite. Volatiles were removed to afford the product as a red-brown microcrystalline solid (170.6 mg, 0.1345 mmol, 95% yield). X-ray quality crystals were grown by slow evaporation of a pentane solution of the compound into toluene at −35 °C. ^{1}H NMR (C_6D_6, 400 MHz, δ): 8.67 (d, J = 8.5 Hz, 4H, anth), 7.79 (d, J = 8.6 Hz, 4H, anth), 7.49 (dd, J = 8.2, 1.1 Hz, 2H, Py), 7.24−7.17 (m, 6H), 7.15−7.07 (m, 6H), 6.35 (dd, J = 7.3, 1.1 Hz, 2H, Py), 1.43−1.20 (m, 48H, THF, SiiPr$_3$), 0.02 (s, 18H), −2.31 (d, $^2J_{YH}$ = 2.1 Hz, 4H, CH_2SiMe_3). ^{13}C NMR (C_6D_6, 101 MHz, δ): 157.87 (Py), 156.52 (Py), 141.25 (pyrr), 138.69, 134.21 (Py), 132.85 (anth), 130.18 (anth), 128.86, 126.81, 125.94 (anth), 122.16 (Py), 119.35, 118.86 (Py), 112.20 (pyrr), 104.14 (−C≡C−), 103.74 (−C≡C−), 71.19 (THF), 29.41 (d, $^1J_{YC}$ = 31.0 Hz, CH_2SiMe_3), 24.50 (THF), 19.15 ($SiCH(CH_3)_2$), 11.83 ($SiCH(CH_3)_2$), 4.32 ($SiCH_3$). Satisfactory elemental analysis could not be obtained for this complex.

Preparation of 13. A Schlenk tube was charged with a stirbar, **12** (34.5 mg, 0.0272 mmol), trimethylsilylacetylene (25 μL, 0.180 mmol), and benzene (4 mL) in the glovebox. This was sealed, brought out of the glovebox, heated to 55 °C for 75 min, then cooled to room temperature, and brought back into the glovebox where volatiles were removed in vacuo. The crude reaction mixture was fractionated over Celite between pentane and benzene, and removal of volatiles from the benzene fraction afforded the product as an orange solid (27.2 mg, 0.0211 mmol, 79%). ^{1}H NMR (C_6D_6, 400 MHz, δ): 8.76 (m, 4H, anth), 8.01 (m, 4H, anth), 7.40 (m, 4H, anth), 7.28 (m, 4H, anth), 7.19 (dd, J = 0.95, 8.13 Hz, 2H, Py), 6.96 (s, 2H, pyrr), 6.91 (dd, J = 7.48, 0.69 Hz, 2H, Py), 6.25 (dd, J = 0.98, 7.34 Hz, 2H, Py), 1.48 (br m, 4H, THF), 1.30 (m, 42H, SiiPr$_3$), 1.00 (br m, 4H, THF), 0.04 (s, 18H, $SiMe_3$). ^{13}C NMR (C_6D_6, 101 MHz, δ) 171.37 (d, J_{YC} = 48.83 Hz, Y−C≡CSiMe$_3$), 157.02 (Py), 156.42 (Py), 140.91 (pyrr), 138.42 (Py), 133.94 (anth), 132.84 (anth), 130.37 (anth), 129.28 (anth), 127.66 (anth), 127.55 (anth), 125.90 (anth), 122.50 (Py), 119.49 (anth), 118.53 (Py), 111.84 (pyrr), 108.28 (d, J_{YC} = 8.42 Hz, Y−C≡C−SiMe$_3$), 104.02 (−C≡C−SiiPr$_3$), 103.98 (−C≡C−SiiPr$_3$), 72.17 (THF), 24.54 (THF), 19.13 ($Si(CH(CH_3)_2)_3$), 11.84 ($Si(CH(CH_3)_2)_3$), 1.69 ($SiMe_3$). Satisfactory elemental analysis could not be obtained for this complex.

Preparation of 14. A solution of indole (15.9 mg, 0.136 mmol) in toluene (2 mL) was added dropwise to a thawing solution of **12** (86.4 mg, 0.0681 mmol) in toluene (2 mL). The solution was stirred for 35 min until warmed, and then volatiles were removed under reduced pressure. The resulting orange solids were washed with pentane and ether and then extracted with benzene to afford the desired complex as a yellow-orange solid (50.8 mg, 0.0405 mmol, 59%). X-ray quality crystals were grown by slow evaporation of a pentane solution of the complex into toluene at −35 °C. ^{1}H NMR (C_6D_6, 400 MHz, δ): 8.47 (br m, 4H, anth), 7.43 (d, J = 6.5 Hz, 2H, Ind), 7.12 (dd, J = 8.1, 0.8 Hz, 2H, Py), 7.07 (s, 2H, pyrr), 7.05 (t, J = 7.4 Hz, 2H, Ind), 6.89−6.76 (m, 8H, anth, Py, Ind), 6.46 (m, 4H, anth), 6.33−6.22 (m, 4H, anth), 5.98 (dd, J = 7.4, 1.0 Hz, 2H, Py), 5.81 (br s, 2H, Ind), 5.13 (br s, 2H, Ind), 1.43 (m, 42 H). ^{13}C NMR (C_6D_6, 101 MHz, δ): 158.62 (Py), 156.23 (Py), 143.01, 141.61 (pyrr), 139.94 (Py), 132.19, 130.80, 129.71, 129.33, 126.34, 126.08, 123.76, 123.37, 120.53, 119.74, 119.48, 118.09, 117.86, 112.58 (pyrr), 104.66 (−C≡C−), 103.63 (−C≡C−), 102.38, 19.29 ($SiCH(CH_3)_2$), 12.03 ($SiCH(CH_3)_2$). Anal calcd. for $C_{80}H_{78}N_5Si_2Y$: C, 76.59; H, 6.27; N, 5.58. Found: C, 76.12; H, 6.39; N, 5.79.

Preparation of 16. $Ti(NMe_2)_4$ (0.03 mL, 0.13 mmol) was added at once to a solution of **4** (57.7 mg, 0.126 mmol) in 3 mL of toluene and stirred for 2.5 days. Volatiles were removed, and the resulting red-orange solids were washed with pentane and then extracted with benzene to afford the product as a red-orange powder (70.0 mg, 0.110 mmol, 87% yield). Crystals

DOI: 10.1021/acsomega.9b01788
ACS Omega 2019, 4, 15879−15892

suitable for X-ray diffraction were grown by vapor diffusion of pentane into a toluene solution of the compound. ^{1}H NMR (C_6D_6, 400 MHz, δ): 7.33 (dd, 2H, Py), 7.24 (s, 2H, pyrr), 7.13 (apparent t, 2H, Py), 6.82 (s, mes, 4H), 6.52 (dd, Py, 2H), 2.77 (s, N(CH_3)$_2$, 18H), 2.16 (s, mes-CH_3, 6H), 2.01 (s, mes-CH_3, 12 H). ^{13}C NMR (C_6D_6, 101 MHz, δ): 159.34 (Py), 155.72 (Py), 144.43 (Pyrr), 138.48 (mes), 136.54 (mes), 136.27 (Py), 135.78 (mes), 128.21 (mes), 120.54 (Py), 117.48 (Py), 113.39 (Pyrr), 45.19 (N(CH_3)$_2$), 20.75 (mes-CH_3), 20.18 (mes-CH_3). Anal calcd. for $C_{38}H_{48}N_6Ti$: C, 71.68; H, 7.60; N, 13.20. Found: C, 71.40; H, 7.50; N, 13.04.

Preparation of 17. Ti(NMe_2)$_4$ (0.13 mL, 0.55 mmol) was added at once to a suspension of **5** (325.8 mg, 0.568 mmol) in 6 mL of toluene and stirred for 2 days. Volatiles were removed, and the resulting orange solids were triturated with pentane, then collected by filtration, and washed with fresh pentane to afford the product as an orange powder (381.2 mg, 0.506 mmol, 92% yield). ^{1}H NMR (C_6D_6, 400 MHz, δ): 8.18 (s, 2H, anth), 7.82−7.79 (m, 8H, anth), 7.42 (dd, J = 8.1, 1.0 Hz, 2H, Py), 7.26 (s, 2H, pyrr), 7.24−7.20 (m, 4H, anth), 7.15−7.10 (m, 6H, anth, Py), 6.71 (dd, J = 7., 1.0 Hz, Py), 2.39 (s, 18H, N(CH_3)$_2$). ^{13}C NMR (C_6D_6, 101 MHz, δ): 157.67 (Py), 156.41 (Py), 145.06 (pyrr), 136.54 (anth), 136.50 (Py), 131.91 (anth), 130.60 (anth), 128.52 (anth), 127.47 (anth), 125.52 (anth), 125.34 (anth), 123.04 (Py), 118.62 (Py), 116.40 (anth), 114.27 (pyrr), 45.16 (N(CH_3)$_2$). Satisfactory elemental analysis could not be obtained for this complex.

Preparation of 18. A solution of **4** (63.2 mg, 0.138 mmol) in 3 mL of toluene was added at once to a solution of Zr(NMe_2)$_4$ (40.2 mL, 0.150 mmol) in 2 mL of toluene and stirred for 30 min. Volatiles were removed, and the resulting yellow solids were triturated with pentane, then collected on a frit, and washed with fresh pentane to afford the product as an yellow powder (85.0 mg, 0.125 mmol, 91% yield). ^{1}H NMR (C_6D_6, 400 MHz, δ): 7.33 (d, J = 7.9 Hz, 2H, Py), 7.19 (s, 2H, pyrr), 7.14 (dd, J = 7.6 Hz, 2H, Py), 6.81 (s, 4H, mes), 6.55 (dd, J = 7.4 Hz, 2H, Py), 2.60 (s, 18H, N(CH_3)$_2$), 2.14 (s, 18H, mesCH_3). ^{13}C (C_6D_6, 101 MHz, δ): 159.59 (Py), 155.47 (Py), 143.95 (pyrr), 138.02 (mes), 137.17 (mes), 137.03 (Py), 136.41 (mes), 128.70 (mes), 121.08 (Py), 117.56 (Py), 114.44 (pyrr), 41.96 (N(CH_3)$_2$), 21.11 (mesCH_3), 20.58 (mesCH_3). Anal calcd. for $C_{38}H_{48}N_6Zr$: C, 67.11; H, 7.11; N, 12.36. Found: C, 66.73; H, 6.93; N, 12.07.

Preparation of 19. A suspension of **5** (320.5 mg, 0.559 mmol) in 5 mL of toluene was added at once to a solution of Zr(NMe_2)$_4$ (150.5 mg, 0.5626 mmol, 1 equiv) in 2 mL of toluene and stirred for 2 days. Volatiles were removed, and the resulting yellow solids were triturated with pentane, collected by filtration, and washed with fresh pentane to afford the product as a yellow powder (398.10 mg, 0.500 mmol, 89% yield). ^{1}H NMR (C_6D_6, 400 MHz, δ): 8.14 (s, 2H, anth), 7.85 (m, 4H, anth), 7.77 (m, 4H, anth), 7.44 (d, J = 8.1 Hz, 2H, Py), 7.23−7.14 (m, 8H, anth, pyrr, Py), 7.10 (m, 4H, anth), 6.75 (dd, Py), 2.12 (s, 18H, N(CH_3)$_2$). ^{13}C NMR (C_6D_6, 101 MHz, δ): 157.65 (Py), 155.87 (Py), 144.08 (pyrr), 137.02 (Py), 135.59 (anth), 131.85 (anth), 130.69 (anth), 128.53 (anth), 127.93 (anth), 127.24 (anth), 125.65 (anth), 125.28 (anth), 123.21 (Py), 118.28 (Py), 114.88 (pyrr), 41.51 (N(CH_3)$_2$). Satisfactory elemental analysis could not be obtained for this complex.

Preparation of 20. A solution of **4** (52.1, 0.114 mmol) in 1.5 mL of toluene was added at once to a solution of Hf(NMe_2)$_4$ (45.2 mg, 0.127 mmol) in 2 mL of toluene and stirred for 30 min. Volatiles were removed, and the resulting yellow solids were washed with pentane and then extracted with benzene to afford the product as a yellow powder (80.5 mg, 0.105 mmol, 92% yield). ^{1}H NMR (C_6D_6, 400 MHz, δ): 7.32 (d, J = 8.0 Hz, 2H, Py), 7.16 (s, 2H, pyrr), 7.13 (apparent t, J = 7.94 Hz, 2H, Py), 6.82 (S, 4H, mes), 6.56 (d, J = 7.4 Hz, 2H, Py), 2.63 (s, 18H, NMe_2), 2.15 (s, 18H, mesCH_3). ^{13}C (C_6D_6, 101 MHz, δ): 159.82 (Py), 155.21 (Py), 144.27 (pyrr), 137.98 (mes), 137.19 (mes), 137.13 (Py), 136.38 (mes), 128.73 (mes), 128.59 (mes), 121.39 (Py), 117.62 (Py), 114.86 (pyrr), 41.62 (NCH_3), 21.11 (mesCH_3), 20.58 (mesCH_3). Anal calcd. for $C_{38}H_{48}N_6Hf$: C, 59.48; H, 6.31; N, 10.95. Found: C, 59.93; H, 6.30; N, 10.47.

Preparation of 21. A solution of **5** (48.1 mg, 0.0838 mmol) in 2 mL of toluene was added at once to a solution of Hf(NMe_2)$_4$ (34.0 mg, 0.0959 mmol) in 1.5 mL of toluene and stirred for 2 days. Volatiles were removed, and the resulting yellow solids were washed with pentane and then extracted with benzene to afford the product as a yellow powder (61.1 mg, 0.0692 mmol, 83% yield). ^{1}H NMR (C_6D_6, 400 MHz, δ): 8.15 (s, 2H, anth), 7.85 (m, 4H, anth), 7.78 (m, 4H, anth), 7.42 (d, J = 7.9 Hz, 2H, Py), 7.22−7.18 (m, 6H, anth and pyrr), 7.18−7.06 (m, 6H, anth, Py), 6.75 (d, J = 7.2 Hz, 2H, Py), 2.16 (s, 18H, N(CH_3)$_2$). ^{13}C NMR (C_6D_6, 101 MHz, δ): 157.85 (Py), 155.60 (Py), 144.47 (pyrr), 137.11 (Py), 135.54 (anth), 131.86 (anth), 130.69 (anth), 128.46 (anth), 127.98 (anth), 127.21 (anth), 125.66 (anth), 125.28 (anth), 123.50 (Py), 118.34 (Py), 115.32 (pyrr), 41.18 (N(CH_3)$_2$). Satisfactory analysis could not be obtained for this complex.

General Small-Scale Polymerization Procedure. In the glovebox, a Fisher-Porter bottle was charged with PhCl (7 mL), 1-hexene (0 or 0.50 mL, 0 or 4.0 mmol, 0 or 1000 equiv), $AlMe_3$ (0.08 mL, 0.8 mmol, 200 equiv), and [CPh_3][B(C_6F_5)$_4$] (2 mL of 33.3 mg in 6 mL PhCl stock solution, 3 equiv) and sealed. A syringe was charged with the desired precatalyst (0.004 mmol in 1 mL PhCl, 1 equiv) and sealed. Both were brought out of the glovebox, the Fisher-Porter bottle was charged with 40 PSI ethylene, the precatalyst solution was injected, and the pressure rapidly increased to 100 PSI. After the desired reaction time, ethylene flow was stopped and pressure vented, and the reaction was quenched by slow addition of 10% HCl in MeOH solution (v/v). Solids were triturated in at least 50 mL of 10% HCl in MeOH for several hours, then collected by filtration, washed with additional fresh 10% HCl in MeOH, and dried under vacuum.

General Large-Scale Polymerization Procedure. Polymerizations were carried out in a 500 mL Büchi glass autoclave using a HiTech polymerization reactor system. The reactor vessel was heated to 110 °C under high vacuum for several minutes and then purged repeatedly with Ar and vacuum to remove air and moisture. Upon cooling of the vessel under Ar to the desired reaction temperature (60 or 80 °C), the vessel was charged with MAO (7.5 mL, 1000 equiv) and PhMe (100 mL) and presaturated with ethylene (5 bar) for 10 min. For ethylene-1-hexene copolymerizations, the reaction was additionally charged with 1-hexene (20 mL, 1600 equiv) prior to presaturation. Upon presaturation, the precatalyst (0.01 mmol) in PhMe (10 mL) was injected into the reactor. The reaction was stirred for 60 min at 5 bar ethylene pressure and 60 or 80 °C; ethylene consumption was monitored by a mass flow controller (Brooks Instrument). After the desired reaction time, ethylene flow was stopped and excess pressure was vented. The polymerization was quenched by addition of 5%

DOI: 10.1021/acsomega.9b01788
ACS Omega 2019, 4, 15879−15892

HCl in MeOH (200 mL), and the resulting polymer was isolated by filtration, washed with fresh methanol, and dried under high vacuum.

GPC Analysis. Gel permeation chromatographic (GPC) analysis of polymers was performed at 160 °C (PL-GPC 220, Agilent Technologies) equipped with two PLgel Olexis 300 × 7.5 mm columns. BHT (0.0125 wt %) was added to 1,2,4-trichlorobenzene to prevent polymer sample degredation. Sample solutions of 2.5−3.0 mg/1.5 mL were prepared at 140 °C, and 100 μL was injected into the GPC. Data was analyzed using the Cirrus software package, and the GPC was calibrated using polystyrene standards. The polystyrene calibration curve was converted into the universal using the Mark−Houwink constants of polystyrene (K = 0.000406 dL/g and α = 0.725).[44]

DSC Analysis. Differential scanning calorimetric (DSC) analysis was performed using a DSC Q2000 (TA Instruments). The temperature and heat flow of the instrument were calibrated with an indium standard. Polymer samples were first equilibrated at 25 °C, followed by heating to 200 °C at a rate of 10 °C/min under N_2 flow (50 mL/min). The temperature was maintained at 200 °C for 5 min, and then the samples were cooled to 25 °C at a rate of 10 °C/min. The temperature was maintained at 25 °C for 5 min, and then samples were reheated to 200 °C at a rate of 10 °C/min. The melting temperature (T_M) for each sample was determined from the second heating scan. The percent crystallinity was calculated from ΔH_f(J/g)/ΔH(J/g), where ΔH_{std} is the heat of fusion for a perfectly crystalline polyethylene (290.0 J/g).[45]

■ ASSOCIATED CONTENT

Supporting Information

The Supporting Information is available free of charge on the ACS Publications website at DOI: 10.1021/acsomega.9b01788.

X-ray crystallographic details for compounds **8**, **11**, **12**, **14**, **15**, and **16** (CIF)

Tables of polymerization trials, supplementary figures for NMR and polymer characterization, and crystallographic details (PDF)

■ AUTHOR INFORMATION

Corresponding Author

*E-mail: agapie@caltech.edu.

ORCID

Theodor Agapie: 0000-0002-9692-7614

Present Address

§Current address: Department of Chemistry, Princeton University, Princeton, New Jersey 08544, United States

Notes

The authors declare no competing financial interest.

■ ACKNOWLEDGMENTS

Mike Takase and Larry Henling are acknowledged for crystallographic assistance. The authors are grateful for the support provided by King Fahd University of Petroleum and Minerals, Dhahran, Saudi Arabia, offered under the KFUPM-Caltech Research Collaboration.

■ REFERENCES

(1) (a) Shook, R. L.; Borovik, A. S. Role of the secondary coordination sphere in metal-mediated dioxygen activation. *Inorg. Chem.* **2010**, *49*, 3646−3660. (b) Cook, S. A.; Borovik, A. S. Molecular designs for controlling the local environments around metal ions. *Acc. Chem. Res.* **2015**, *48*, 2407−2414. ((c)) Moore, C. M.; Szymczak, N. K. Appended Functionality in Pincer Ligands. In *Pincer and Pincer-Type Complexes*; Szabo, K. J.; Wendt, O. F. Eds.; Wiley-VCH: Weinheim, Germany, 2014; pp 71−94. (d) Hale, L. V. A.; Szymczak, N. K. Hydrogen Transfer Catalysis beyond the Primary Coordination Sphere. *ACS Catal.* **2018**, *8*, 6446−6461.

(2) (a) Shirin, Z.; Hammes, B. S.; Young, V. G.; Borovik, A. S. Hydrogen Bonding in Metal Oxo Complexes: Synthesis and Structure of a Monomeric Manganese(III)-Oxo Complex and Its Hydroxo Analogue. *J. Am. Chem. Soc.* **2000**, *122*, 1836−1837. (b) MacBeth, C. E.; Gupta, R.; Mitchell-Koch, K. R.; Young, V. G., Jr.; Lushington, G. H.; Thompson, W. H.; Hendrich, M. P.; Borovik, A. S. Utilization of hydrogen bonds to stabilize M-O(H) units: synthesis and properties of monomeric iron and manganese complexes with terminal oxo and hydroxo ligands. *J. Am. Chem. Soc.* **2004**, *126*, 2556−2567. (c) Borovik, A. S. Bioinspired hydrogen bond motifs in ligand design: the role of noncovalent interactions in metal ion mediated activation of dioxygen. *Acc. Chem. Res.* **2005**, *38*, 54−61. (d) Shook, R. L.; Peterson, S. M.; Greaves, J.; Moore, C.; Rheingold, A. L.; Borovik, A. S. Catalytic reduction of dioxygen to water with a monomeric manganese complex at room temperature. *J. Am. Chem. Soc.* **2011**, *133*, 5810−5817. (e) Han, Z.; Horak, K. T.; Lee, H. B.; Agapie, T. Tetranuclear Manganese Models of the OEC Displaying Hydrogen Bonding Interactions: Application to Electrocatalytic Water Oxidation to Hydrogen Peroxide. *J. Am. Chem. Soc.* **2017**, *139*, 9108−9111. (f) Wallen, C. M.; Palatinus, L.; Bacsa, J.; Scarborough, C. C. Hydrogen Peroxide Coordination to Cobalt(II) Facilitated by Second-Sphere Hydrogen Bonding. *Angew. Chem., Int. Ed.* **2016**, *55*, 11902−11906. (g) Wallen, C. M.; Bacsa, J.; Scarborough, C. C. Coordination of Hydrogen Peroxide with Late-Transition-Metal Sulfonamido Complexes. *Inorg. Chem.* **2018**, *57*, 4841−4848. (h) Dahl, E. W.; Kiernicki, J. J.; Zeller, M.; Szymczak, N. K. Hydrogen Bonds Dictate O_2 Capture and Release within a Zinc Tripod. *J. Am. Chem. Soc.* **2018**, *140*, 10075−10079. (i) Dahl, E. W.; Dong, H. T.; Szymczak, N. K. Phenylamino derivatives of tris(2-pyridylmethyl)amine: hydrogen-bonded peroxodicopper complexes. *Chem. Commun.* **2018**, *54*, 892−895.

(3) Moore, C. M.; Szymczak, N. K. Nitrite reduction by copper through ligand-mediated proton and electron transfer. *Chem. Sci.* **2015**, *6*, 3373−3377.

(4) (a) Franco, F.; Cometto, C.; Ferrero Vallana, F.; Sordello, F.; Priola, E.; Minero, C.; Nervi, C.; Gobetto, R. A local proton source in a [Mn(bpy-R)$(CO)_3$Br]-type redox catalyst enables CO_2 reduction even in the absence of Brønsted acids. *Chem. Commun.* **2014**, *50*, 14670−14673. (b) Franco, F.; Cometto, C.; Nencini, L.; Barolo, C.; Sordello, F.; Minero, C.; Fiedler, J.; Robert, M.; Gobetto, R.; Nervi, C. Local Proton Source in Electrocatalytic CO_2 Reduction with [Mn(bpy-R)$(CO)_3$Br] Complexes. *Chem. − Eur. J.* **2017**, *23*, 4782−4793.

(5) (a) Moore, C. M.; Szymczak, N. K. A tris(2-quinolylmethyl)-amine scaffold that promotes hydrogen bonding within the secondary coordination sphere. *Dalton Trans.* **2012**, *41*, 7886−7889. (b) Geri, J. B.; Szymczak, N. K. A Proton-Switchable Bifunctional Ruthenium Complex That Catalyzes Nitrile Hydroboration. *J. Am. Chem. Soc.* **2015**, *137*, 12808−12814. (c) Dahl, E. W.; Szymczak, N. K. Hydrogen Bonds Dictate the Coordination Geometry of Copper: Characterization of a Square-Planar Copper(I) Complex. *Angew. Chem., Int. Ed.* **2016**, *55*, 3101−3105.

(6) (a) Kiernicki, J. J.; Zeller, M.; Szymczak, N. K. Hydrazine Capture and N-N Bond Cleavage at Iron Enabled by Flexible Appended Lewis Acids. *J. Am. Chem. Soc.* **2017**, *139*, 18194−18197. (b) Kiernicki, J. J.; Zeller, M.; Szymczak, N. K. Requirements for Lewis Acid-Mediated Capture and N-N Bond Cleavage of Hydrazine at Iron. *Inorg. Chem.* **2019**, *58*, 1147−1154.

DOI: 10.1021/acsomega.9b01788
ACS Omega 2019, 4, 15879−15892

(7) (a) Miller, A. J. M.; Labinger, J. A.; Bercaw, J. E. Reductive coupling of carbon monoxide in a rhenium carbonyl complex with pendant Lewis acids. *J. Am. Chem. Soc.* **2008**, *130*, 11874−11875. (b) Miller, A. J. M.; Labinger, J. A.; Bercaw, J. E. Homogeneous CO Hydrogenation: Ligand Effects on the Lewis Acid-Assisted Reductive Coupling of Carbon Monoxide. *Organometallics* **2010**, *29*, 4499−4516.
(8) Tseng, K.-N. T.; Kampf, J. W.; Szymczak, N. K. Modular Attachment of Appended Boron Lewis Acids to a Ruthenium Pincer Catalyst: Metal-Ligand Cooperativity Enables Selective Alkyne Hydrogenation. *J. Am. Chem. Soc.* **2016**, *138*, 10378−10381.
(9) Ostapowicz, T. G.; Merkens, C.; Hölscher, M.; Klankermayer, J.; Leitner, W. Bifunctional ruthenium(II) hydride complexes with pendant strong Lewis acid moieties: structure, dynamics, and cooperativity. *J. Am. Chem. Soc.* **2013**, *135*, 2104−2107.
(10) Creutz, S. E.; Peters, J. C. Exploring secondary-sphere interactions in Fe-N_xH_y complexes relevant to N_2 fixation. *Chem. Sci.* **2017**, *8*, 2321−2328.
(11) Rakowski DuBois, M.; DuBois, D. L. Development of molecular electrocatalysts for CO_2 reduction and H_2 production/oxidation. *Acc. Chem. Res.* **2009**, *42*, 1974−1982.
(12) (a) Khosrowabadi Kotyk, J. F.; Ziller, J. W.; Yang, J. Y. Copper tetradentate N_2Py_2 complexes with pendant bases in the secondary coordination sphere: improved ligand synthesis and protonation studies. *J. Coord. Chem.* **2015**, *69*, 1990−2002. (b) Khosrowabadi Kotyk, J. F.; Hanna, C. M.; Combs, R. L.; Ziller, J. W.; Yang, J. Y. Intramolecular hydrogen-bonding in a cobalt aqua complex and electrochemical water oxidation activity. *Chem. Sci.* **2018**, *9*, 2750−2755.
(13) Tutusaus, O.; Ni, C.; Szymczak, N. K. A transition metal Lewis acid/base triad system for cooperative substrate binding. *J. Am. Chem. Soc.* **2013**, *135*, 3403−3406.
(14) (a) He, L.; Ma, D.; Duan, L.; Wei, Y.; Qiao, J.; Zhang, D.; Dong, G.; Wang, L.; Qiu, Y. Control of intramolecular $\pi-\pi$ stacking interaction in cationic iridium complexes via fluorination of pendant phenyl rings. *Inorg. Chem.* **2012**, *51*, 4502−4510. (b) Mashita, T.; Tsushima, S.; Takao, K. Controlling the lability of uranyl(vi) through intramolecular $\pi-\pi$ stacking. *Dalton Trans.* **2018**, *47*, 13072−13080. (c) Qu, Z. Z.; Gao, T. B.; Wen, J.; Rui, K.; Ma, H.; Cao, D. K. Cyclometalated Ir(III) complexes $[Ir(tpy)(bbibH_2)Cl][PF_6]$ and $[Ir(tpy)(bmbib)Cl][PF_6]$: intramolecular π-π interactions leading to facile synthesis and enhanced luminescence. *Dalton Trans.* **2018**, *47*, 9779−9786. (d) Pandey, I. K.; Natarajan, M.; Faujdar, H.; Hussain, F.; Stein, M.; Kaur-Ghumaan, S. Intramolecular stabilization of a catalytic [FeFe]-hydrogenase mimic investigated by experiment and theory. *Dalton Trans.* **2018**, *47*, 4941−4949. (e) Blindauer, C. A.; Griesser, R.; Holý, A.; Operschall, B. P.; Sigel, A.; Song, B.; Sigel, H. Intramolecular π-stacks in mixed-ligand copper(II) complexes formed by heteroaromatic amines and antivirally active acyclic nucleotide analogs carrying a hydroxy-2-(phosphonomethoxy)propyl residue. *J. Coord. Chem.* **2018**, *71*, 1910−1934. (f) Congrave, D. G.; Hsu, Y. T.; Batsanov, A. S.; Beeby, A.; Bryce, M. R. Sky-blue emitting bridged diiridium complexes: beneficial effects of intramolecular $\pi-\pi$ stacking. *Dalton Trans.* **2018**, *47*, 2086−2098. (g) Namanga, J. E.; Gerlitzki, N.; Smetana, V.; Mudring, A. V. Supramolecularly Caged Green-Emitting Ionic Ir(III)-Based Complex with Fluorinated C^N Ligands and Its Application in Light-Emitting Electrochemical Cells. *ACS Appl. Mater. Interfaces* **2018**, *10*, 11026−11036. (h) Shih, W.-C.; Chiang, Y.-T.; Wang, Q.; Wu, M.-C.; Yap, G. P. A.; Zhao, L.; Ong, T.-G. Invisible Chelating Effect Exhibited between Carbodicarbene and Phosphine through $\pi-\pi$ Interaction and Implication in the Cross-Coupling Reaction. *Organometallics* **2017**, *36*, 4287−4297. (i) Congrave, D. G.; Hsu, Y.-t.; Batsanov, A. S.; Beeby, A.; Bryce, M. R. Synthesis, Diastereomer Separation, and Optoelectronic and Structural Properties of Dinuclear Cyclometalated Iridium(III) Complexes with Bridging Diarylhydrazide Ligands. *Organometallics* **2017**, *36*, 981−993. (j) Martinez, C. R.; Iverson, B. L. Rethinking the term "pi-stacking". *Chem. Sci.* **2012**, *3*, 2191−2201. (k) Meyer, E. A.; Castellano, R. K.; Diederich, F. Interactions with Aromatic Rings in Chemical and Biological Recognition. *Angew. Chem., Int. Ed.* **2003**, *42*, 1210−1250. (l) Kobayashi, M.; Hayakawa, N.; Matsuo, T.; Li, B.; Fukunaga, T.; Hashizume, D.; Fueno, H.; Tanaka, K.; Tamao, K. (Z)-1,2-Di(1-pyrenyl)disilene: Synthesis, Structure, and Intramolecular Charge-Transfer Emission. *J. Am. Chem. Soc.* **2016**, *138*, 758−761. (m) Wang, Z.; Yang, H.; He, P.; He, Y.; Zhao, J.; Tang, H. A highly-efficient blue-light excitable red phosphor: intramolecular π-stacking interactions in one dinuclear europium(iii) complex. *Dalton Trans.* **2016**, *45*, 2839−2844. (n) Schneider, G. E.; Pertegás, A.; Constable, E. C.; Housecroft, C. E.; Hostettler, N.; Morris, C. D.; Zampese, J. A.; Bolink, H. J.; Junquera-Hernández, J. M.; Ortí, E.; Sessolo, M. Bright and stable light-emitting electrochemical cells based on an intramolecularly π-stacked, 2-naphthyl-substituted iridium complex. *J. Mater. Chem. C* **2014**, *2*, 7047−7055. (o) Li, P.; Shan, G. G.; Cao, H. T.; Zhu, D. X.; Su, Z. M.; Jitchati, R.; Bryce, M. R. Intramolecular π Stacking in Cationic Iridium(III) Complexes with Phenyl-Functionalized Cyclometalated Ligands: Synthesis, Structure, Photophysical Properties, and Theoretical Studies. *Eur. J. Inorg. Chem.* **2014**, *2014*, 2376−2382. (p) Costa, R. D.; Casillas, R.; Cano, J. Do the Intramolecular π Interactions Improve the Stability of Ionic, Pyridine-Carbene-Based Iridium(III) Complexes? *J. Phys. Chem. C* **2013**, *117*, 8545−8555. (q) Fraser, M. G.; van der Salm, H.; Cameron, S. A.; Blackman, A. G.; Gordon, K. C. Heteroleptic Cu(I) bis-diimine complexes of 6,6'-dimesityl-2,2'-bipyridine: a structural, theoretical and spectroscopic study. *Inorg. Chem.* **2013**, *52*, 2980−92.
(15) Barboiu, M.; Prodi, L.; Montalti, M.; Zaccheroni, N.; Kyritsakas, N.; Lehn, J.-M. Dynamic Chemical Devices: Modulation of Photophysical Properties by Reversible, Ion-Triggered, and Proton-Fuelled Nanomechanical Shape-Flipping Molecular Motions. *Chem. − Eur. J.* **2004**, *10*, 2953−2959.
(16) Barboiu, M.; Legrand, Y.-M.; Prodi, L.; Montalti, M.; Zaccheroni, N.; Vaughan, G.; van der Lee, A.; Petit, E.; Lehn, J.-M. Modulation of Photochemical Properties in Ion-Controlled Multicomponent Dynamic Devices. *Eur. J. Inorg. Chem.* **2009**, 2621−2628.
(17) (a) Wang, S.-Y.; Fu, J.-H.; Liang, Y.-P.; He, Y.-J.; Chen, Y.-S.; Chan, Y.-T. Metallo-Supramolecular Self-Assembly of a Multicomponent Ditrigon Based on Complementary Terpyridine Ligand Pairing. *J. Am. Chem. Soc.* **2016**, *138*, 3651−3654. (b) He, Y.-J.; Tu, T.-H.; Su, M.-K.; Yang, C.-W.; Kong, K. V.; Chan, Y.-T. Facile Construction of Metallo-supramolecular Poly(3-hexyltiophene)-*block*-Poly(ethylene oxide) Diblock Copolymers via Complementary Coordination and Their Self-Assembled Nanostructures. *J. Am. Chem. Soc.* **2017**, *139*, 4218−4224.
(18) (a) Brauchli, S. Y.; Constable, E. C.; Harris, K.; Häussinger, D.; Housecroft, C. E.; Rösel, P. J.; Zampese, J. A. Towards catenanes using π-stacking interactions and their influence on the spin-state of a bis(2,2′:6′,2″-terpyridine)iron(II) domain. *Dalton Trans.* **2010**, *39*, 10739−10748. (b) Pelascini, F.; Wesolek, M.; Peruch, F.; Cian, A. D.; Kyritsakas, N.; Lutz, P. J.; Kress, J. Iron complexes of terdentate nitrogen ligands: formation and X-ray structure of three new dicationic complexes. *Polyhedron* **2004**, *23*, 3193−3199.
(19) (a) Onoda, A.; Kawakita, K.; Okamura, T.-A.; Yamamoto, H.; Ueyama, N. (Acetonitrile)(6,6″-dimesityl-2,2′:6′,2″-terpyridine)-copper(I) hexafluorophosphate. *Acta Crystallogr., Sect. E: Struct. Rep.Online* **2003**, *59*, m266. (b) Constable, E. C.; Edwards, A. J.; Haire, G. R.; Hannon, M. J.; Raithby, P. R. Silver(I)-2,2′:6′2′-terpyridine complexes: X-ray structure of $[\{Ag(tpy)(MeCN)\}_2][PF_6]_2$ and $[Ag(dptpy)(MeCN)][BF_4]$·MeCN (tpy = 2,2′: 6′2′-terpyridine; dptpy = 6,6′-diphenyl-2,2′:6′,2′-terpyridine). *Polyhedron* **1998**, *17*, 243−253. (c) Onoda, A.; Kawakita, K.; Okamura, T.; Yamamoto, H.; Ueyama, N. A distorted square-planar Pd^{II} complex with a shortened Pd-Cl bond induced by the bulky terpyridyl ligand 6,6″-dimesityl-2,2′:6′,2′′-terpyridine. *Acta Crystallogr., Sect. E: Struct. Rep. Online* **2003**, *59*, m291. (d) Kamata, K.; Suzuki, A.; Nakai, Y.; Nakazawa, H. Catalytic Hydrosilylation of Alkenes by Iron Complexes Containing Terpyridine Derivatives as Ancillary Ligands. *Organometallics* **2012**, *31*, 3825−3828.
(20) (a) Kulangara, S. V.; Jabri, A.; Yang, Y.; Korobkov, I.; Gambarotta, S.; Duchateau, R. Synthesis, X-ray Structural Analysis,

DOI: 10.1021/acsomega.9b01788
ACS Omega 2019, 4, 15879−15892

and Ethylene Polymerization Studies of Group IV Metal Heterobimetallic Aluminum-Pyrrolyl Complexes. *Organometallics* **2012**, *31*, 6085−6094. (b) Dias, A. R.; Ferreira, A. P.; Veiros, L. F. Bonding Geometry of Pyrrolyl in Zirconium Complexes: Fluxionality between σ and π Coordination. *Organometallics* **2003**, *22*, 5114−5125. (c) Dias, A. R.; Veiros, L. F. Are cyclopentadienyl complexes more stable than their pyrrolyl analogues? *J. Organomet. Chem.* **2005**, *690*, 1840−1844. ((d)) Heys, P. N.; Odedra, R.; Kingsley, A.; Davies, H. O. Hafnium and zirconium pyrrolyl-based organometallic precursors and their use for preparing dielectric thin films. WO2009155520A1, 2009. (e) Hsu, J.-W.; Lin, Y.-C.; Hsiao, C.-S.; Datta, A.; Lin, C.-H.; Huang, J.-H.; Tsai, J.-C.; Hsu, W.-C. Zirconium complexes incorporated with asymmetrical tridentate pincer type mono- and di-anionic pyrrolyl ligands: mechanism and reactivity as catalytic precursors. *Dalton Trans.* **2012**, *41*, 7700−7707. (f) Huang, J.-H.; Kuo, P.-C.; Lee, G.-H.; Peng, S.-M. Synthesis and structure characterization of 2-(dimethylaminomethyl)pyrrolate and 2,5-bis-(dimethylaminomethyl)pyrrolate zirconium complexes. *J. Chin. Chem. Soc.* **2000**, *47*, 1191−1195. (g) Kaushik, N. K.; Bhushan, B.; Sodhi, G. S. Dithiocarbazate complexes of titanium(IV), zirconium(IV) and oxomolybdenum(VI) derivatives. *Indian J. Chem., Sect. A: Inorg. Phys. Theor. Anal.* **1981**, *20A*, 625−626. (h) Sodhi, G. S.; Kaushik, N. K. Oxinate chelates of cyclopentadienyl- or indenylzirconium(IV) and their halide salts. *Bull. Soc. Chim. Fr.* **1982**, 45−48. (i) Sodhi, G. S.; Kumar, S.; Kaushik, N. K. Dithiocarbamate anions as salts of oxinate chelates of zirconium(IV). *Acta Chim. Hung.* **1983**, *114*, 329−335. (j) Sharma, A. K.; Kaushik, N. K. Syntheses of (π-fluorenyl) and (π-pyrrolyl)thallium(I) and their group transfer reactions with trichloro-(π-cyclopentadienyl)titanium(IV)/trichloro(π-cyclopentadienyl)-zirconium(IV). *Acta Chim. Hung.* **1984**, *116*, 361−365. ((k)) Zhao, W.; Xu, X.; Yi, J.; Jing, X.; Chen, W. Olefin polymerization catalysts of Group IV metal complexes with pyrrole ring-containing ligands. CN1317500A, 2001. (l) Korobkov, I.; Gambarotta, S. Unusual Reactivity of a Tm-Pyrrolide/Aluminate Complex with a Metallocene-Type Structural Motif. *Organometallics* **2009**, *28*, 5560−5567. (m) Nikiforov, G. B.; Crewdson, P.; Gambarotta, S.; Korobkov, I.; Budzelaar, P. H. M. Reduction of Titanium Supported by a σ-/π-Bonded Tripyrrole Ligand: Ligand C−N Bond Cleavage and Coordination of Olefin and Arene with an Inverse Sandwich Structure. *Organometallics* **2007**, *26*, 48−55. (n) Novak, A.; Blake, A. J.; Wilson, C.; Love, J. B. Titanium and zirconium complexes supported by dipyrrolide ligands. *Chem. Commun.* **2002**, 2796−2797. (o) Tanski, J. M.; Parkin, G. Synthesis and Structures of Zirconium−Pyrrolyl Complexes: Computational Analysis of the Factors That Influence the Coordination Modes of Pyrrolyl Ligands. *Organometallics* **2002**, *21*, 587−589. (p) Billow, B. S.; McDaniel, T. J.; Odom, A. L. Quantifying ligand effects in high-oxidation-state metal catalysis. *Nat. Chem.* **2017**, *9*, 837−842. (q) Ferreira da Silva, J. L.; Galvão, A. C.; Ferreira, A. P.; Galvão, A. M.; Dias, A. R.; Gomes, P. T.; Salema, M. S. Effect of ancillary ligands in the hapticity of the pyrrolyl ligand in [Ti(pyrrolyl)(NMe2)xCl3−x] (x=0, 1, 2, 3) complexes. *J. Organomet. Chem.* **2010**, *695*, 1533−1540. (r) Swartz, D. L., II; Odom, A. L. Effects of 5,5-substitution on dipyrrolylmethane ligand isomerization. *Dalton Trans.* **2008**, 4254−4258.

(21) (a) Dawson, D. M.; Walker, D. A.; Thornton-Pett, M.; Bochmann, M. Synthesis and reactivity of sterically hindered iminopyrrolato complexes of zirconium, iron, cobalt and nickel. *J. Chem. Soc., Dalton Trans.* **2000**, 459−466. (b) Yasumoto, T.; Yamagata, T.; Mashima, K. Olefin Polymerization Catalyst Derived by Activation of a Neutral Monoalkyl Titanium Complex with an Aminopyrrole Ligand Using Triisobutylaluminum and Trityl Borate. *Chem. Lett.* **2007**, *36*, 1030−1031. (c) Yoshida, Y.; Matsui, S.; Takagi, Y.; Mitani, M.; Nakano, T.; Tanaka, H.; Kashiwa, N.; Fujita, T. New Titanium Complexes Having Two Pyrrolide−Imine Chelate Ligands: Syntheses, Structures, and Ethylene Polymerization Behavior. *Organometallics* **2001**, *20*, 4793−4799. (d) Tsurugi, H.; Mashima, K. Preparation and Characterization of a Zwitterionic (Iminopyrrolyl) zirconium Complex with Benzylaluminate Anion and Its Catalytic Performance for 1-Hexene Polymerization. *Organometallics* **2006**, *25*, 5210−5212. (e) Yasumoto, T.; Yamagata, T.; Mashima, K. Isoselective Living Polymerization of 1-Hexene Catalyzed by Half-Metallocene Dimethyl Complexes of Hafnium with Bidentate N-Substituted (Iminomethyl)pyrrolyl Ligands. *Organometallics* **2005**, *24*, 3375−3377. (f) Yoshida, Y.; Mohri, J.; Ishii, S.; Mitani, M.; Saito, J.; Matsui, S.; Makio, H.; Nakano, T.; Tanaka, H.; Onda, M.; Yamamoto, Y.; Mizuno, A.; Fujita, T. Living copolymerization of ethylene with norbornene catalyzed by bis(pyrrolide-imine) titanium complexes with MAO. *J. Am. Chem. Soc.* **2004**, *126*, 12023−12032. (g) Tsurugi, H.; Matsuo, Y.; Yamagata, T.; Mashima, K. Intramolecular Benzylation of an Imino Group of Tridentate 2,5-Bis(N-aryliminomethyl)pyrrolyl Ligands Bound to Zirconium and Hafnium Gives Amido-Pyrrolyl Complexes That Catalyze Ethylene Polymerization. *Organometallics* **2004**, *23*, 2797−2805. (h) Pinheiro, A. C.; da Silva, S. M.; Roisnel, T.; Kirillov, E.; Carpentier, J. F.; Casagrande, O. L. Synthesis and structural characterization of zirconium complexes supported by tridentate pyrrolide-imino ligands with pendant N-, O- and S-donor groups and their application in ethylene polymerization. *New J. Chem.* **2018**, *42*, 1477−1483. (i) Yasumoto, T.; Yamamoto, K.; Tsurugi, H.; Mashima, K. Isospecific polymerization of 1-hexene by C_1-symmetric half-metallocene dimethyl complexes of group 4 metals with bidentate N-substituted iminomethylpyrrolyl ligands. *Dalton Trans.* **2013**, *42*, 9120−9128. (j) Pennington, D. A.; Coles, S. J.; Hursthouse, M. B.; Bochmann, M.; Lancaster, S. J. Salicylaldiminato Pyrrolylaldiminato Group 4 Metal Alkene Polymerization Catalysts: Combining High Activity with High Comonomer Incorporation. *Macromol. Rapid Commun.* **2006**, *27*, 599−604. (k) Yoshida, Y.; Matsui, S.; Fujita, T. Bis(pyrrolide-imine) Ti complexes with MAO: A new family of high performance catalysts for olefin polymerization. *J. Organomet. Chem.* **2005**, *690*, 4382−4397. (l) Mashima, K.; Tsurugi, H. Uniqueness and versatility of iminopyrrolyl ligands for transition metal complexes. *J. Organomet. Chem.* **2005**, *690*, 4414−4423. (m) Matsui, S.; Yoshida, Y.; Takagi, Y.; Spaniol, T. P.; Okuda, J. Pyrrolide-imine benzyl complexes of zirconium and hafnium: synthesis, structures, and efficient ethylene polymerization catalysis. *J. Organomet. Chem.* **2004**, *689*, 1155−1164. (n) Yoshida, Y.; Nakano, T.; Tanaka, H.; Fujita, T. Catalytic Behavior of Bis(Pyrrolide-Imine) and Bis(Phenoxy-Imine) Titanium Complexes for the Copolymerization of Ethylene with Propylene, 1-Hexene, or Norbornene. *Isr. J. Chem.* **2002**, *42*, 353−359. (o) Yoshida, Y.; Matsui, S.; Takagi, Y.; Mitani, M.; Nitabaru, M.; Nakano, T.; Tanaka, H.; Fujita, T. Post-Metallocenes: New Bis(pyrrolyl-2-aldiminato) Titanium Complexes for Ethylene Polymerization. *Chem. Lett.* **2000**, *29*, 1270−1271. (p) Li, G.; Lamberti, M.; Mazzeo, M.; Pappalardo, D.; Pellecchia, C. Isospecific polymerization of propene by new indolyl-pyridylamido Zr(IV) catalysts. *J. Mol. Catal. A: Chem.* **2013**, *370*, 28−34. (q) Li, G.; Lamberti, M.; D'Amora, S.; Pellecchia, C. C_1-Symmetric Pentacoordinate Anilidopyridylpyrrolide Zirconium(IV) Complexes as Highly Isospecific Olefin Polymerization Catalysts. *Macromolecules* **2010**, *43*, 8887−8891. (r) Annunziata, L.; Pappalardo, D.; Tedesco, C.; Pellecchia, C. Isotactic-Specific Polymerization of Propene by a *Cs*-Symmetric Zirconium(IV) Complex Bearing a Dianionic Tridentate [$^-$NNN$^-$] Amidomethylpyrrolidepyridine Ligand. *Macromolecules* **2009**, *42*, 5572−5578. (s) Li, G.; Lamberti, M.; Roviello, G.; Pellecchia, C. New Titanium and Hafnium Complexes Bearing [−NNN−] Pyrrolylpyridylamido Ligands as Olefin Polymerization Catalysts. *Organometallics* **2012**, *31*, 6772−6778. (t) Li, G.; Zuccaccia, C.; Tedesco, C.; D'Auria, I.; Macchioni, A.; Pellecchia, C. NMR spectroscopy and X-ray characterisation of cationic a further level of complexity for the elusive active species of pyridylamido olefin polymerisation catalysts. *Chem. − Eur. J.* **2014**, *20*, 232−244. (u) Broomfield, L. M.; Sarazin, Y.; Wright, J. A.; Hughes, D. L.; Clegg, W.; Harrington, R. W.; Bochmann, M. Mixed-ligand iminopyrrolato-salicylaldiminato group 4 metal complexes: Optimising catalyst structure for ethylene/propylene copolymerisations. *J. Organomet. Chem.* **2007**, *692*, 4603−4611. (v) Pennington, D. A.; Coles, S. J.; Hursthouse, M. B.; Bochmann, M.; Lancaster, S. J. Hybrid catalysts: the synthesis, structure and ethene polymerisation activity of

DOI: 10.1021/acsomega.9b01788
ACS Omega 2019, 4, 15879−15892

(salicylaldiminato)(pyrrolylaldiminato) titanium complexes. *Chem. Commun.* **2005**, 3150−3152.
(22) (a) Hu, X.-H.; Liang, Y.; Li, C.; Yi, X.-Y. Multi-nuclear silver(I) and copper(I) complexes: a novel bonding mode for bispyridylpyrrolides. *Dalton Trans.* **2014**, *43*, 2458−2464. (b) Wang, Y.-P.; Hu, X.-H.; Wang, Y.-F.; Pan, J.; Yi, X.-Y. The syntheses, characterization and photophysical properties of phosphine copper(I) and silver(I) complexes with the bispyridylpyrrolide ligand. *Polyhedron* **2015**, *102*, 782−787.
(23) (a) Tabatchnik-Rebillon, A.; Aubé, C.; Bakkali, H.; Delaunay, T.; Manh, G. T.; Blot, V.; Thobie-Gautier, C.; Renault, E.; Soulard, M.; Planchat, A.; le Questel, J.-Y.; Le Guével, R.; Guguen-Guillouzo, C.; Kauffmann, B.; Ferrand, Y.; Huc, I.; Urgin, K.; Condon, S.; Léonel, E.; Evain, M.; Lebreton, J.; Jacquemin, D.; Pipelier, M.; Dubreuil, D. Electrochemical Synthesis and Characterisation of Alternating Tripyridyl-Dipyrrole Molecular Strands with Multiple Nitrogen-Based Donor-Acceptor Binding Sites. *Chem. − Eur. J.* **2010**, *16*, 11876−11889 S11876/1-S11876/17; . (b) Balewski, Ł.; Sączewski, F.; Bednarski, P.; Gdaniec, M.; Borys, E.; Makowska, A. Structural diversity of copper(II) complexes with N-(2-pyridyl)-imidazolidin-2-ones(thiones) and their in vitro antitumor activity. *Molecules* **2014**, *19*, 17026−17051. (c) Samanta, S. K.; Rana, A.; Schmittel, M. Reversible cargo shipping between orthogonal stations of a nanoscaffold upon redox input. *Dalton Trans.* **2014**, *43*, 9438−47. (d) Wang, Y.-P.; Xiao, J.-J.; Hu, X.-H.; Yi, X.-Y. Syntheses and structures of neutral dicopper(I) halide complexes with bispyridylpyrrole ligand. *Inorg. Chim. Acta* **2015**, *435*, 125−130. (e) Min, R.; Hu, X.-h.; Yi, X.-y.; Zhang, S.-c. Synthesis, structure, DNA binding and cleavage activity of a new copper(II) complex of bispyridylpyrrolide. *J. Cent. South Univ. (Engl. Ed.)* **2015**, *22*, 1619−1625. (f) Fang, W.-Z.; Wang, Y.-P.; Wang, Y.-F.; Zhang, S.-C.; Yi, X.-Y. Anion-directed assembly of helical copper(II) complexes based on a bispyridylpyrrole ligand: synthesis, structural and magnetic properties. *RSC Adv.* **2015**, *5*, 8996−9001.
(24) (a) Alam, M. S.; Stocker, M.; Gieb, K.; Müller, P.; Haryono, M.; Student, K.; Grohmann, A. Spin-State Patterns in Surface-Grafted Beads of Iron(II) Complexes. *Angew. Chem. Int. Ed.* **2010**, *49*, 1159−1163. (b) Frazier, B. A.; Williams, V. A.; Wolczanski, P. T.; Bart, S. C.; Meyer, K.; Cundari, T. R.; Lobkovsky, E. B. C-C Bond Formation and Related Reactions at the CNC Backbone in (smif)FeX (smif = 1,3-Di-(2-pyridyl)-2-azaallyl): Dimerizations, 3 + 2 Cyclization, and Nucleophilic Attack; Transfer Hydrogenations and Alkyne Trimerization (X = $N(TMS)_2$, dpma = (Di-(2-pyridyl-methyl)-amide)). *Inorg. Chem.* **2013**, *52*, 3295−3312. (c) Bowman, D. N.; Bondarev, A.; Mukherjee, S.; Jakubikova, E. Tuning the Electronic Structure of Fe(II) Polypyridines via Donor Atom and Ligand Scaffold Modifications: A Computational Study. *Inorg. Chem.* **2015**, *54*, 8786−8793.
(25) (a) Yan, L.; Seminario, J. M. Electronic Structure and Electron Transport Characteristics of a Cobalt Complex. *J. Phys. Chem. A* **2005**, *109*, 6628−6633. ((b)) Liu, Y.; Liang, H.; Chen, Z.; Qin, Q.; Xu, Q.; Jiang, Y. Method for synthesis of cobalt(II) metal complex using oxojsoaporphincs derivative as ligand for use in preparation of anti-tumor drug. CN104370908A, 2015. (c) Qin, Q.-P.; Qin, J.-L.; Meng, T.; Lin, W.-H.; Zhang, C.-H.; Wei, Z.-Z.; Chen, J.-N.; Liu, Y.-C.; Liang, H.; Chen, Z.-F. High in vivo antitumor activity of cobalt oxoisoaporphine complexes by targeting G-quadruplex DNA, telomerase and disrupting mitochondrial functions. *Eur. J. Med. Chem.* **2016**, *124*, 380−392. (d) McPherson, J. N.; Hogue, R. W.; Akogun, F. S.; Bondì, L.; Luis, E. T.; Price, J. R.; Garden, A. L.; Brooker, S.; Colbran, S. B. Predictable Substituent Control of $Co^{III/II}$ Redox Potentials and Spin Crossover in Bis(dipyridylpyrrolide)cobalt Complexes. *Inorg. Chem.* **2019**, *58*, 2218−2228.
(26) (a) McSkimming, A.; Diachenko, V.; London, R.; Olrich, K.; Onie, C. J.; Bhadbhade, M. M.; Bucknall, M. P.; Read, R. W.; Colbran, S. B. An Easy One-Pot Synthesis of Diverse 2,5-Di(2-pyridyl)pyrroles: A Versatile Entry Point to Metal Complexes of Functionalised, Meridial and Tridentate 2,5-Di(2-pyridyl)pyrrolato Ligands. *Chem. − Eur. J.* **2014**, *20*, 11445−11456. ((b)) Nomura, K.; Sato, H.; Kobayashi, K. Photoelectric conversion element, dye-sensitized solar cell, metal complex dye, and dye solution made by dissolving metal complex dye. WO2014050578A1, 2014. ((c)) Nomura, K.; Sato, H.; Kobayashi, K.; Watanabe, K. Photoelectric conversion element and dye-sensitized solar cell. WO2014050528A1, 2014. (d) Zhong, Y.-Q.; Xiao, H.-Q.; Yi, X.-Y. Synthesis, structural characterization and catalysis of ruthenium(II) complexes based on 2,5-bis(2′-pyridyl)-pyrrole ligand. *Dalton Trans.* **2016**, *45*, 18113−18119.
(27) McPherson, J. N.; Abad Galan, L.; Iranmanesh, H.; Massi, M.; Colbran, S. B. Synthesis and structural, redox and photophysical properties of tris-(2,5-di(2-pyridyl)pyrrolide) lanthanide complexes. *Dalton Trans.* **2019**, *48*, 9365−9375.
(28) Imler, G. H.; Lu, Z.; Kistler, K. A.; Carroll, P. J.; Wayland, B. B.; Zdilla, M. J. Complexes of 2,5-Bis(α-pyridyl)pyrrolate with Pd(II) and Pt(II): A Monoanionic Iso-π-Electron Ligand Analog of Terpyridine. *Inorg. Chem.* **2012**, *51*, 10122−10128.
(29) Chen, J.-J.; Gan, Z.-L.; Huang, Q.; Yi, X.-Y. Well-defined dinuclear silver phosphine complexes based on nitrogen donor ligand and their high efficient catalysis for A3-coupling reaction. *Inorg. Chim. Acta* **2017**, *466*, 93−99.
(30) Zhang, Z.; Lim, J. M.; Ishida, M.; Roznyatovskiy, V. V.; Lynch, V. M.; Gong, H. Y.; Yang, X.; Kim, D.; Sessler, J. L. Cyclo[m]-pyridine[n]pyrroles: hybrid macrocycles that display expanded π-conjugation upon protonation. *J. Am. Chem. Soc.* **2012**, *134*, 4076−4079.
(31) (a) Usui, K.; Tanoue, K.; Yamamoto, K.; Shimizu, T.; Suemune, H. Synthesis of substituted azulenes via Pt(II)-catalyzed ring-expanding cycloisomerization. *Org. Lett.* **2014**, *16*, 4662−4665. (b) Natarajan, P.; Schmittel, M. ON-OFF luminescence signaling of hybrid organic-inorganic switches. *Inorg. Chem.* **2013**, *52*, 8579−8590.
(32) de Montigny, F.; Argouarch, G.; Lapinte, C. New Route to Unsymmetrical 9,10-Disubstituted Ethynylanthracene Derivatives. *Synthesis* **2006**, 293−298.
(33) Wannere, C. S.; Schleyer, P. V. R. How do ring currents affect ^{1}H NMR chemical shifts? *Org. Lett.* **2003**, *5*, 605−608.
(34) Addison, A. W.; Rao, T. N.; Reedijk, J.; van Rijn, J.; Verschoor, G. C. Synthesis, structure, and spectroscopic properties of copper(II) compounds containing nitrogen−sulphur donor ligands; the crystal and molecular structure of aqua[1,7-bis(N-methylbenzimidazol-2′-yl)-2,6-dithiaheptane]copper(II) perchlorate. *J. Chem. Soc., Dalton Trans.* **1984**, 1349−1356.
(35) Yang, L.; Powell, D. R.; Houser, R. P. Structural variation in copper(I) complexes with pyridylmethylamide ligands: structural analysis with a new four-coordinate geometry index, τ4. *Dalton Trans.* **2007**, 955−964.
(36) WebElements.com (accessed November 26, 2018).
(37) Kaneko, H.; Dietrich, H. M.; Schädle, C.; Maichle-Mössmer, C.; Tsurugi, H.; Törnroos, K. W.; Mashima, K.; Anwander, R. Synthesis of Rare-Earth-Metal Iminopyrrolyl Complexes from Alkyl Precursors: Ln→Al N-Ancillary Ligand Transfer. *Organometallics* **2013**, *32*, 1199−1208.
(38) Imai, Y. N.; Inoue, Y.; Nakanishi, I.; Kitaura, K. Cl-pi interactions in protein-ligand complexes. *Protein Sci.* **2008**, *17*, 1129−1137.
(39) Pangborn, A. B.; Giardello, M. A.; Grubbs, R. H.; Rosen, R. K.; Timmers, F. J. Safe and Convenient Procedure for Solvent Purification. *Organometallics* **1996**, *15*, 1518−1520.
(40) (a) Bradley, D. C.; Thomas, I. M. 765. Metallo-organic compounds containing metal−nitrogen bonds. Part I. Some dialkylamino-derivatives of titanium and zirconium. *J. Chem. Soc.* **1960**, 3857−3861. (b) Chisholm, M. H.; Hammond, C. E.; Huffman, J. C. Tetrakisdimethylamidozirconium and its dimethylamido lithium adduct: Structures of [zr(nme2)4]2 and zr(nme2)6li2(thf)2. *Polyhedron* **1988**, *7*, 2515−2520. (c) Diamond, G. M.; Rodewald, S.; Jordan, R. F. Efficient Synthesis of rac-(Ethylenebis(indenyl))ZrX_2 Complexes via Amine Elimination. *Organometallics* **1995**, *14*, 5−7.
(41) (a) Chandra, G.; Lappert, M. F. Amido-derivatives of metals and metalloids. Part VI. Reactions of titanium(IV), zirconium(IV), and hafnium(IV) amides with protic compounds. *J. Chem. Soc. A*

DOI: 10.1021/acsomega.9b01788
ACS Omega 2019, 4, 15879−15892

1968, *1968*, 1940−1945. (b) Diamond, G. M.; Jordan, R. F.; Petersen, J. L. Synthesis of Group 4 Metal *rac*-(EBI)M(NR_2)$_2$ Complexes by Amine Elimination. Scope and Limitations. *Organometallics* **1996**, *15*, 4030−4037.

(42) (a) Estler, F.; Eickerling, G.; Herdtweck, E.; Anwander, R. Organo-Rare-Earth Complexes Supported by Chelating Diamide Ligands. *Organometallics* **2003**, *22*, 1212−1222. (b) Arndt, S.; Voth, P.; Spaniol, T. P.; Okuda, J. Dimeric Hydrido Complexes of Rare-Earth Metals Containing a Linked Amido−Cyclopentadienyl Ligand: Synthesis, Characterization, and Monomer−Dimer Equilibrium. *Organometallics* **2000**, *19*, 4690−4700. (c) Lappert, M. F.; Pearce, R. Stable silylmethyl and neopentyl complexes of scandium(III) and yttrium(III). *J. Chem. Soc., Chem. Commun.* **1973**, *1973*, 126.

(43) (a) Anwander, R.; Runte, O.; Eppinger, J.; Gerstberger, G.; Herdtweck, E.; Spiegler, M. Synthesis and structural characterisation of rare-earth bis(dimethylsilyl)amides and their surface organometallic chemistry on mesoporous MCM-41. *J. Chem. Soc., Dalton Trans.* **1998**, *1998*, 847−858. (b) Herrmann, W. A.; Anwander, R.; Munck, F. C.; Scherer, W.; Dufaud, V.; Huber, N. W.; Artus, G. R. J. Lanthanoid Complexes, IX [1]. Reactivity Control of Lanthanoid Amides through Ligand Effects: Synthesis and Structures of Sterically Congested Alkoxy Complexes. *Z. Naturforsch., B: J. Chem. Sci.* **1994**, *49*, 1789−1797.

(44) Atiqullah, M.; Moman, A. A.; Akhtar, M. N.; Al-Muallem, H. A.; Abu-Raqabah, A. H.; Ahmed, N. Supported SiO_2-^{n}BuSnCl_3/MAO/(^{n}BuCp)$_2$ZrCl_2 catalyzing MAO cocatalyst-free ethylene polymerization: Study of hydrogen responsiveness. *J. Appl. Polym. Sci.* **2007**, *106*, 3149−3157.

(45) Dias, P.; Lin, Y. J.; Poon, B.; Chen, H. Y.; Hiltner, A.; Baer, E. Adhesion of statistical and blocky ethylene−octene copolymers to polypropylene. *Polymer* **2008**, *49*, 2937−2946.

DOI: 10.1021/acsomega.9b01788
ACS Omega 2019, 4, 15879−15892